Contract/Grant Number AFOSR-87-0299

HOMOGENIZING SURFACE AND SATELLITE OBSERVATIONS OF CLOUD

A. Henderson-Sellers and A.H. Goodman
Department of Geography
University of Liverpool
Liverpool, U.K.

October 1988

Final Scientific Report, 1 October 1987 – 30 September 1988

Prepared for

EUROPEAN OFFICE OF AEROSPACE RESEARCH AND DEVELOPMENT
London, England

REPORT DOCUMENTATION PAGE		READ INSTRUCTIONS BEFORE COMPLETING FORM
1. Report Number EOARD-TR-89-03	2. Govt Accession No.	3. Recipient's Catalog Number
4. Title (and Subtitle) Homogenizing surface and satellite observations of cloud.		5. Type of Report & Period Covered Interim, 1 October 87 30 September 88. 6. Performing Org. Report Number
7. Author(s) Ann Henderson-Sellers and Alan Goodman		8. Contract or Grant Number AFOSR-85-0299
9. Performing Organization Name and Address Department of Geography, University of Liverpool, P.O. Box 147, Liverpool, L69. 3BX.		10. Program Element, Project, Task Area & Work Unit Numbers
11. Controlling Office Name and Address EOARD 223/231 Old Marylebone Road, London, NW1, 5TH U.K.		12. Report Date 1 October 1988 13. Number of Pages 54
14. Monitoring Agency Name and Address		15.
16. & 17. Distribution Statement Approved for public release; distribution unlimited.		
18. Supplementary Notes		
19. Key Words Contingency probability of clouds, probability of occurrence of unseen low-level clouds, observing practice, failure to report marine cirrus, global cloud climatologies.		

20. Abstract

Using four months of global surface cloud observations an investigation has been made concerning both types of contingency probability as applied to different cloud levels. Analysis of the probability of observing an upper cloud given the presence of a lower cloud, P(L→U) with varying lower level cloud amounts gives different results from those of Hahn et al. (1982) at a variety of spatial scales ranging from individual stations to the globe. The implications of this are discussed with respect to the probability of observing a lower cloud in the presence of an upper cloud, P(U→L). We find that their evaluation of P(U→L) is greater than our calculation which is modified to account for the variation in P(L→U). Their overestimate is most noticeable in low and middle latitudes and can be reversed (to an underestimate) in some high

20. Abstract cont,d...../2.

latitude areas.

Plans for the investigations of temporal variations in cloud amount and type on the ocean surface radiation budget are also discussed in the context of the first analysis of the large data set of all-sky camera imagery obtained from the Joint Air Sea Interaction Experiment (JASIN) conducted in 1978. Our results show a considerable temporal variability in total and high cloud amount cf. conventional (bridge) observations. Also we find that the bridge observer often failed to report thin upper-level cloud. This omission, if it is widespread, may also affect the surface-based climatologies of Hahn et al.

This report has been reviewed by the EOARD Information Office and is releasable to the National Technical Information Service (NTIS). At NTIS it will be releasable to the general public, including foreign nations.

This technical report has been reviewed and is approved for publication.

Owen R. Coté

OWEN R. COTE'
Chief, Geophyiscs and Space

Fred T. Gilliam

FRED T. GILLIAM, Lt. Col, USAF
Chief Scientist

Contents

1. Introduction

This is the final scientific report under this grant. It is, however, an abbreviated summary for two reasons. Firstly some of the, very interesting, work undertaken by Alan Goodman on the contingency probabilities of layered clouds has already been reported in the final scientific report under grant AFOSR–87–0195. Additionally it is our intention to provide a more complete report of the whole of this project in the form of a bound copy of Alan Goodman's Ph.D. thesis. This will be forwarded to Dr Coté in due course.

2. Climatological Contingency Probabilities of Clouds

2.1 Introduction

Cloud amounts and types can change rapidly in time and cloud configurations are often multi-layered. One fundamental aspect of any complete cloud climatology is the vertical *association of different cloud types*. This entails establishing the probabilities of co-occurrence of two, or more, cloud types and is equally important for a satellite based cloud climatology as for a surface based climatology since both observing platforms can suffer obscuration of certain cloud layers by intervening clouds.

This study extends that reported in Section 5 of Henderson-Sellers *et al.* (1988) final scientific report to AFGL on "Improved Snow and Cloud Monitoring: New Climatological Relationships between Surface and Satellite Observations".

2.2 Ideas and interdependency of contingency probabilities

Contingency probabilities define the likelihood of observing (from the ground or by satellites) one cloud type, given the presence of another type. Hahn *et al.* (1982) introduced the idea of contingency probabilities in the first of four cloud reports which included maps

depicting the global distribution of contingency probabilities for specific combinations of cloud types. Of particular concern is the need to determine the probability of an upper level cloud existing when there is a lower level overcast. This is because the more useful inverse quantity i.e. the probability of a lower level cloud existing given the presence of an upper level cloud, requires such values in its calcuation and as is shown no direct calculation may be attempted when the lower cloud is overcast.

Hahn *et al.* (1982) investigated the behaviour of the probability of an upper cloud given a lower cloud for the range of lower level cloud amounts (1–7 oktas) and found the situation summarised in their figure 1. Their analysis was for the three months March/April/May (Spring) in the Northern Hemisphere for 1971 and was derived from ocean cloudiness data. They claimed that it showed that the probability of seeing an upper level cloud given a lower level cloud is roughly constant across the range of lower level cloud amounts.

The issue is of considerable importance because the P(U⇒L)quantity is a direct function of the value of P(L⇒U) for the overcast case and also of the number of overcasts. Thus any errors in the estimation of P(L⇒U) for obscured levels will be manifest to an extent as errors in the P(U⇒L) calculations. It therefore seems worthwhile to investigate the way in which observable upper cloud (i.e. in the cases of lower cloud amounts in the range 1 to 7 oktas) probabilities vary.

2.3 Observations of probabilities of upper level cloud co-occurrence with low level cloud

The data source used were the global surface weather observations for the months of July 1983, July 1986, January 1985 and January 1987. These contain information on the

types of low, middle and high cloud present according to the WMO classification (WMO, 1974), as well as total and layered cloud amounts. Particular attention is focussed on those cloud type combinations for L and U that were used by Hahn *et al.* (1982).

P(L⇒U)is calculated by dividing the number of times both cloud types were seen together (NBS) by the number of occasions the lower cloud was present and both levels could be observed. This latter quantity is defined by subtracting from the occasions when L was observed (NLS) the number of times the upper level was unreported (NUU) e.g. when the lower level was overcast.

$$P(L \Rightarrow U) = NBS/(NLS - NUU) \quad (1)$$

In order to make the ensuing calculations as representative as possible a threshold defining the minimum number of occasions that the upper level had to be seen in the presence of the lower cloud was used for each analysis. Since calculations were made over the range of lower level cloud amounts the threshold was applied for each lower cloud amount value.

2.3.1 Hemispheric and Global Results

P(L⇒U) was calculated over the range of lower level cloud amounts for L = stratus/stratocumulus and U = i) altostratus/altocumulus and ii) cirriform. For the large scale analysis it was required that for each cloud amount interval both cloud levels had to be reported on at least 40 occasions. Figure 1 illustrates P(L⇒U) behaviour over the globe for all four months data combined. As only half of the months provided oceanic data, analysis is restricted to land-based observations. The left vertical axis relates to the traces of contingency probability whilst the right vertical axis relates to the cloud amount

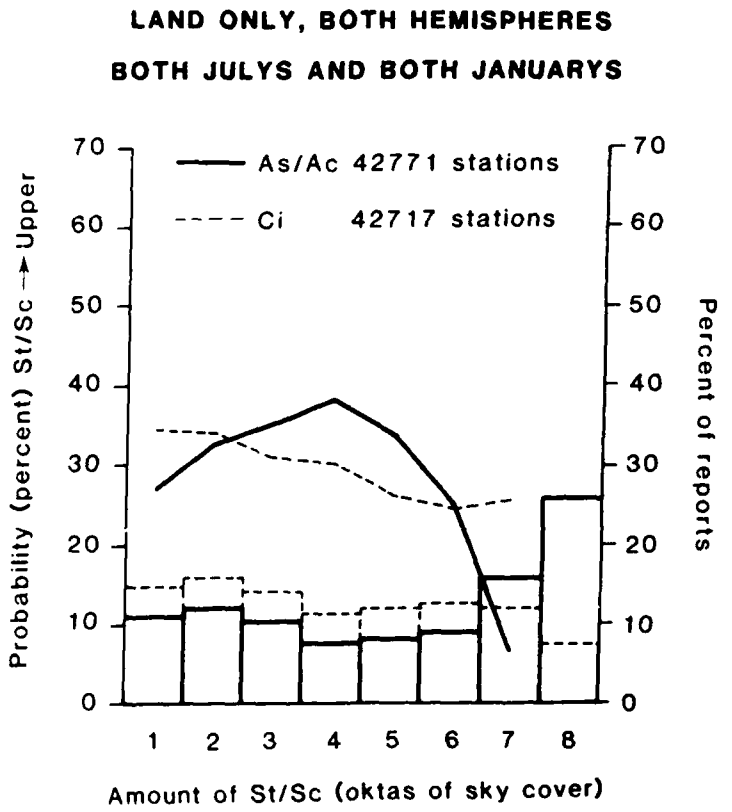

Figure 1 Probability of occurrence of As/Ac and Ci with given amounts of St/Sc over the globe for all four months of data from land-based sources

histogram. The station count is cumulated from all four months data and the total number of occasions both cloud levels were observable (higher for U = altiform cloud) was approaching 2 million.

On a global basis the value of P(L⇒U) varies only slightly from 1–7 oktas low cloud for the stratiform/cirriform case. The mean probability over the non-overcast reports differs from the 6 and 7 okta values by only 3 or 4 percent and the validity of the fundamental principle does not appear to be in much doubt. The stratiform/altiform case shows considerably more variability with a distinct peak at 4 oktas.

The result from all four months data was then "decomposed" into its constituent January and July components. There was little overall difference between the cumulative result and the separate January and July results and the patterns of P(L⇒U) behaviour were well retained with the maximum co-occurrence probability for stratiform/altiform cloud still at four oktas. This result is of particular significance due to the higher frequency of stratiform overcasts.

As the original testing of the fundamental principle, described by Hahn *et al.* (1982) was performed using observations made over the ocean, a separate analysis was carried out on the oceanic component of the data in which both contingency probabilities decreased with increasing lower cloud amount with large numbers of stratiform overcasts reported. Because the oceanic data set was so much smaller than the land component, this leads us to suspect that the Hahn result, having been generated from a relatively small data set has then been applied, perhaps over ambitiously, to much larger volumes of data.

2.3.2 Regional Results and individual Station Analysis

The study was extended to smaller spatial scales to investigate any regional variability within the larger scale trends. A 20 degree latitude by 20 degree longitude grid was set up and the individual boxes sampled in turn for sufficient data. The two January and July monthly pairs were considered separately and a threshold of 20 occasions set as the minimum number of times lower and upper cloud levels had to be reported. This threshold restricted analysis to 30 or so well-sampled boxes mostly over the land areas.

The distinctive feature of the stratiform/cirriform results was the realisation that the global trend appears to be a mean between opposing patterns where the contingency probability both increases and decreases with increasing low cloud amount. Almost as prominent was the tendency for P(L⇒U) to show an increase (sometimes substantial) from 6 to 7 oktas. A typical example of such behaviour is shown in Figure 2. The reasons behind these probability distributions are unclear but a possible clue may be found by referring to the P(L⇒U) formula (Equation (1)). In order for it to increase from one cloud amount interval to another either i) NBS must increase, ii) NLS must decrease or iii) NUU must increase. In progressing from 6 to 7 oktas of stratiform cloud the first two options appear unlikely to be the cause but the value of NUU may rise considerably as a result of observing procedures where slight gaps or suspected gaps are reported as 7 oktas rather than 8. However in such cases the upper level may be unreported thus causing NUU and P(L⇒U) to rise.

It thus appears from our data that at both regional and global scales the value of P(L⇒U) applicable to overcast situations with altiform upper cloud is best represented by the value for 7 oktas rather than by the mean over the non-overcast cloud amount range.

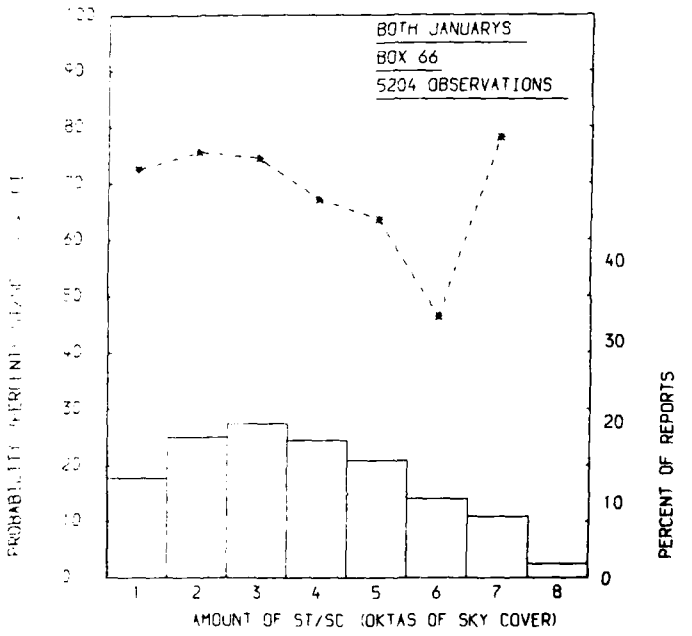

Figure 2 Probability of occurrence of As/Ac with St/Sc for given amounts of St/Sc over box 10°–30°S and 40°–60°E for both Januarys

Where cirrus is concerned, however, the P(L⇒U) figure most appropriate to high level overcasts appears to relate to the location of the observations.

The results from individual stations within selected boxes were then examined in order to see whether the box plots gave an overall representative picture of P(L⇒U) behaviour within an area or were simply the result of many different results in combination with each other. Six of the better sampled boxes from the southern hemispheric mid-latitude, equatorial and northern hemispheric mid-latitude regions were chosen and the data for all four months from ten regularly reporting stations from each box used to construct P(L⇒U) diagrams which were subsequently compared to the appropriate box diagrams.

The stations diagrams showed 'noisier' traces than their box counterparts in the sense that where there was a visible trend in P(L⇒U) between 1 and 7 oktas low cloud it was often half-hidden by spurious peaks. Figure 3, taken from the box 10°N–10°S and 60°–80°W, shows a typical example of such behaviour. This perhaps is not a surprising feature considering the smaller numbers of observations involved. In boxes 135 and 137 although there was sometimes a small deviation in pattern the station plots were generally well correlated with the box plots for both combinations of lower and upper cloud type. In the equatorial and southern mid-latitude boxes the larger scale trend was often still recognisable in the station plots even when masked by noise although unlike boxes 135 and 137 there were odd exceptions of station plots showing opposite trends in P(L⇒U) behaviour from the box plot. Figures 4 to 6, derived from the box 30°–50°S and 60°–80°W, were typical with increased noise arising from the station making fewer observations of both cloud levels.

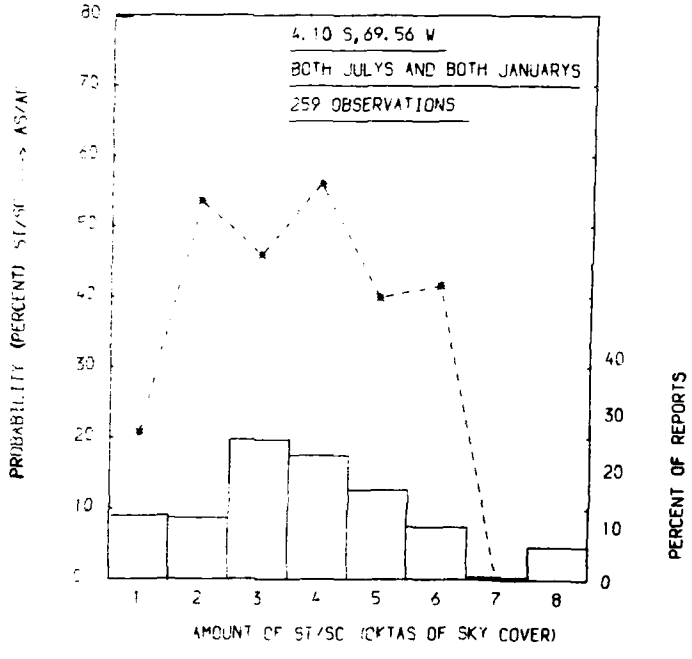

Figure 3 Probability of occurrence of As/Ac with St/Sc for given amounts of St/Sc for the station located at 4°10' S, 69°56'W for both Januarys and both Julys

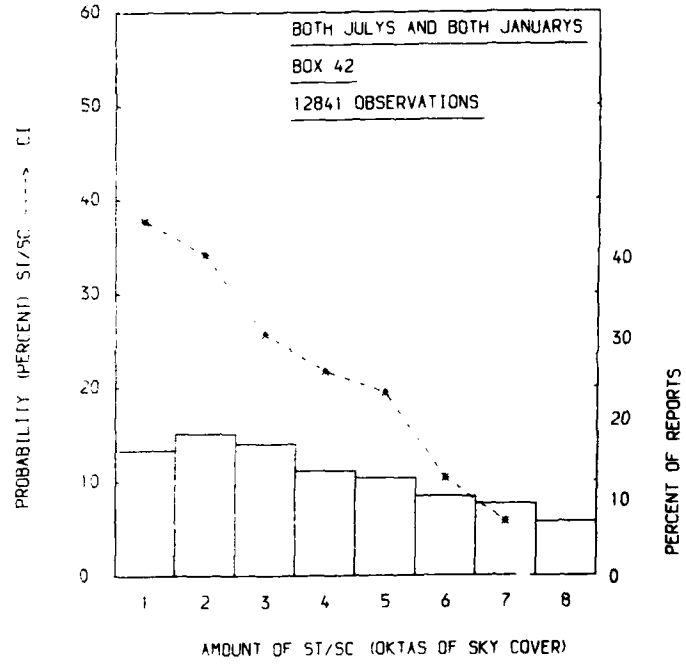

Figure 4 Probability of occurrence of Ci with St/Sc for given amounts of St/Sc over box 30°–50°S and 60°–80°W for both Januarys and both Julys

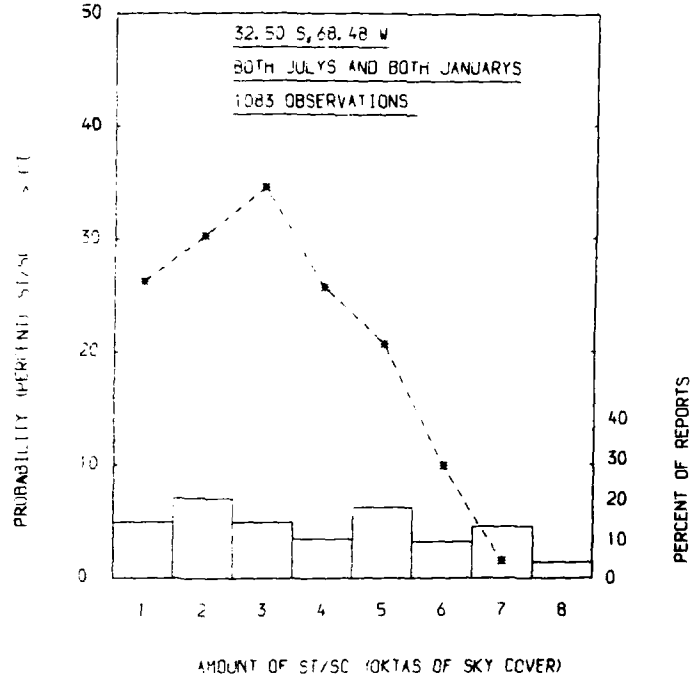

Figure 5 Probability of occurrence of Ci with St/Sc for given amounts of St/Sc for the station located at 32°50' S, 68°48'W for both Januarys and both Julys

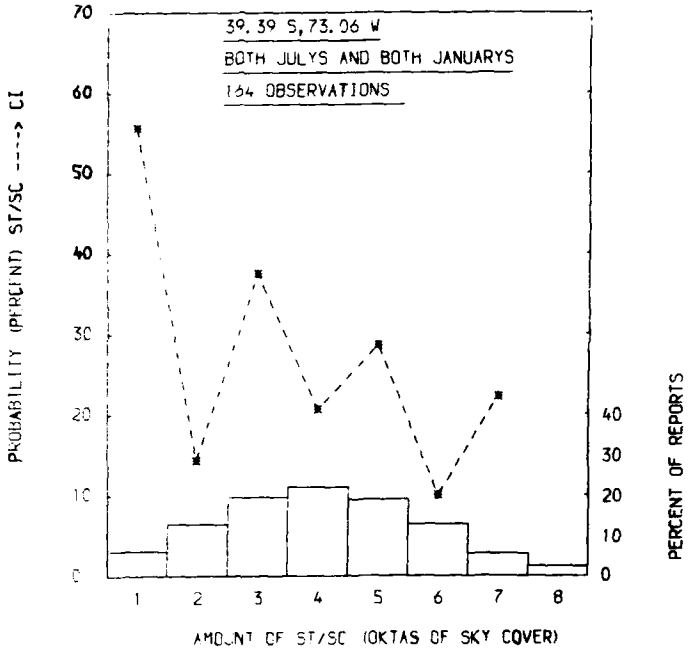

Figure 6 Probability of occurrence of Ci with St/Sc for given amounts of St/Sc for the station located at 39°39' S, 73°06'W for both Januarys and both Julys

2.4 Probability of lower level cloud co-occurrence given upper level overcast: the satellite view

It was demonstrated by Sèze *et al.* (1986) that in a multilayered cloud configuration satellite retrieval algorithms may fail to detect the lowest layers of cloud. One suggested remedy to this potentially serious defect is (on a climatological basis) the use of P(U⇒L) probabilities in which the satellite-retrieved cloud would be referenced as U and climatologies of lower level clouds estimated therefrom. The ideas concerning P(U⇒L) are a direct offshoot from the concerns of P(L⇒U). The most accurate long term values would be required if these probabilities were to be implemented into a climatological satellite retrieval scheme.

2.4.1 Procedure for calculating P(U⇒L)

This calculation is more complex than its counterpart and attention is first focussed upon the numerator. The number of occasions on which both cloud types were seen (NBS) must have added to it the number of times both types would have been seen if the lower cloud had never been overcast. This is given by P(L⇒U) × NUU where NUU, the number of times the upper cloud level was unreported is the identical quantity calculated in Section 2.3. The denominator must contain the total number of times the upper cloud was seen. This must include the number of times it would have been seen if none of the intervening lower clouds had ever been overcast, TNUU (total number upper unreported).

When U is either altostratus or altocumulus TNUU is defined as

$$[P(Cu \Rightarrow U) \times NUU_{Cu}] + [P(Cb \Rightarrow U) \times NUU_{Cb}] + [P(St \Rightarrow U) \times NUU_{St}] \qquad (2)$$

where Cu = cumulus

Cb = cumulonimbus

St = stratus/stratocumulus

and NUU_{St} = number of times the upper level is unreported due to a stratus/stratocumulus overcast etc.

Then,

$$P(U \Rightarrow L) = \frac{NBS + (P(L \Rightarrow U) \times NUU)}{NUS + TNUU} \quad (3)$$

For the case of U = altocumulus/altostratus all the lower clouds are defined as mutually exclusive. However, when U = cirriform type cloud all the lower clouds cannot be said to be mutually exclusive and thus TNUU cannot be estimated by the previous method. Instead, TNUU is approximated as the product of F(Ci) and NHU where F(Ci) is the frequency of occurrence of cirriform cloud calculated from the times when the high cloud level was visible, except for cases of clear sky. NHU, standing for 'number high unreported' is the total number of times the high level was unreported. Then

$$P(U \Rightarrow L) = \frac{NBS + [P(L \Rightarrow U) \times NUU]}{NUS + [F(Ci) \times NHU]} \quad (4)$$

2.4.2 Results and Discussion

The role of the fundamental principle and its logic is apparent in the calculation from the inclusion of the P(L⇒U) terms and the choice of their appropriate values. Consider such a calculation for U = altostratus/altocumulus/cirrus and L = stratus/stratocumulus over some predefined area (e.g. regional, hemispheric). The value of P(L⇒U) used in the numerator will be the mean of all the observations made for 1–7 oktas of stratiform cloud. This is then assumed to be representative of the lower level overcast situation. If the

number of overcast cases is relatively high and the mean value of P(L⇒U) a poor estimator of the 8 oktas situation (as was consistently found for altiform cloud) then the numerator will be biased too high. In the case where cirrus is the upper cloud the resulting P(U⇒L) value may be overestimated to an extent determined by the inaccuracy in P(L⇒U), NUU and to some extent by the relative value of the other terms in the P(U⇒L) equation. When the upper cloud type is altiform it will be noticed that a P(L⇒U) term appears in the denominator as well as the numerator. The resulting bias in P(U⇒L) will then depend on several interrelationships, namely

i) the magnitude of the P(L⇒U) term relative to NBS in the numerator

ii) the influence of the biased P(L⇒U) term on the TNUU parameter in the denominator

iii) the magnitude of the TNUU term relative to the NUS term in the denominator.

It is then difficult to assess the individual effects of single terms within the P(U⇒L) equation with respect to biassing of the resulting value. As part of a general exercise global P(U⇒L) values have been calculated for each of the four months data adopting the fundamental principle as stated by Hahn *et al.* (1982). The next stage was to perform the global calculations again using the modified P(L⇒U) values. For each month the ratio of the value of P(L⇒U) at 7 oktas to the mean value over the 1–7 oktas range of stratiform cloud was calculated and then used in the 'modified' P(U⇒L) calculations. These were then used, along with the original global distributions, to produce P(U⇒L) difference maps (unmodified − modified values) for four selected cloud type combinations.

1) U = Ci L = St/Sc

2) U = As/Ac L = Cu

3) U = As/Ac L = Cb

4) U = As/Ac L = St/Sc

It is suspected that the Hahn climatologies may be in need of some revision to include the times during their ocean and land data series (12 and 10 years respectively) when their fundamental principle was inappropriate.

2.4.3 Comparison of unmodified P(U⇒L) maps with those of Hahn et al.

The monthly data from July 1983 and January 1985 were used to calculate global distributions of P(U⇒L) for eight different combinations of lower and upper cloud type, five of which reference cirriform cloud as the upper type. the remaining three using altiform cloud. To try and ensure a level of representativeness calculations over each resolution area were only made when both levels were visible on 10 or more occasions.

Only land data were used and the probabilities are mapped in divisions of 10%.

1 = 0–10%	6 = 51–60%
2 = 11–20%	7 = 61–70%
3 = 21–30%	8 = 71–80%
4 = 31–40%	9 = 81–90%
5 = 41–50%	10 = 91–100%

Blank spaces are the result of either (i) *no stations* existing within the area, (ii) the 10 observation threshold not being exceeded or (iii) a bogus result having been obtained.

Comparing these maps with those of Hahn *et al.* (1984) highlights the generally higher levels of inter-regional variability or noise found in the monthly plots. This is not a surprising feature as the climatologies generated by Hahn *et al.* have incorporated about two orders of magnitude more data and would be expected to show smoother variations.

However, the greater levels of noise in the monthly porbabilities tend to be encountered in areas where the result is more patchy and thus may not be truly representative. Counter to this is that Hahn *et al.* calculated probabilities to the nearest percent whereas those calculated from the monthly data have been placed in 10% classes which introduces a degree of artificial smoothing by comparison.

Apart from the relative lengths of the data sets, the maps presented by Hahn *et al.* (1984) correspond to three-monthly periods rather than single months. Therefore, in comparing results the assumption is made that their climatologies for December, January and February together are typical for January alone. Similarly, the data for June, July and August are, for purposes here, assumed to be typical of July values.

Monthly values of $P(U \Rightarrow L)$ for cirriform and altiform cloud types respectively (e.g. Figure 7) showed consistent agreement over the greater part of the globe with the Hahn climatologies (Figure 8). Regions of high $P(U \Rightarrow L)$ in the monthly data such as south east Asia are noticeable in the ten-yearly data and the generally good agreement extends to July. Intermonthly variation is apparent in areas such as southern Africa and this increase in $P(U \Rightarrow L)$ from July to January also shows up in the ten year data.

Probabilities involving low level clouds (cumulus, cumulonimbus and particularly stratus/stratocumulus) are of potentially most use if they can improve satellite retrievals of low clouds in the presence of intervening layers. Thus cirriform–stratiform and altiform–stratiform probabilities are of keen interest. Comparison of the former with Hahn *et al.*'s corresponding map (Figures 9 and 10) revealed much similarity in the global pattern. During January the distribution of $P(U \Rightarrow L)$ over Europe, America and Russia is reproduced clearly in the ten year data with repeated agreement found in July where, apart from

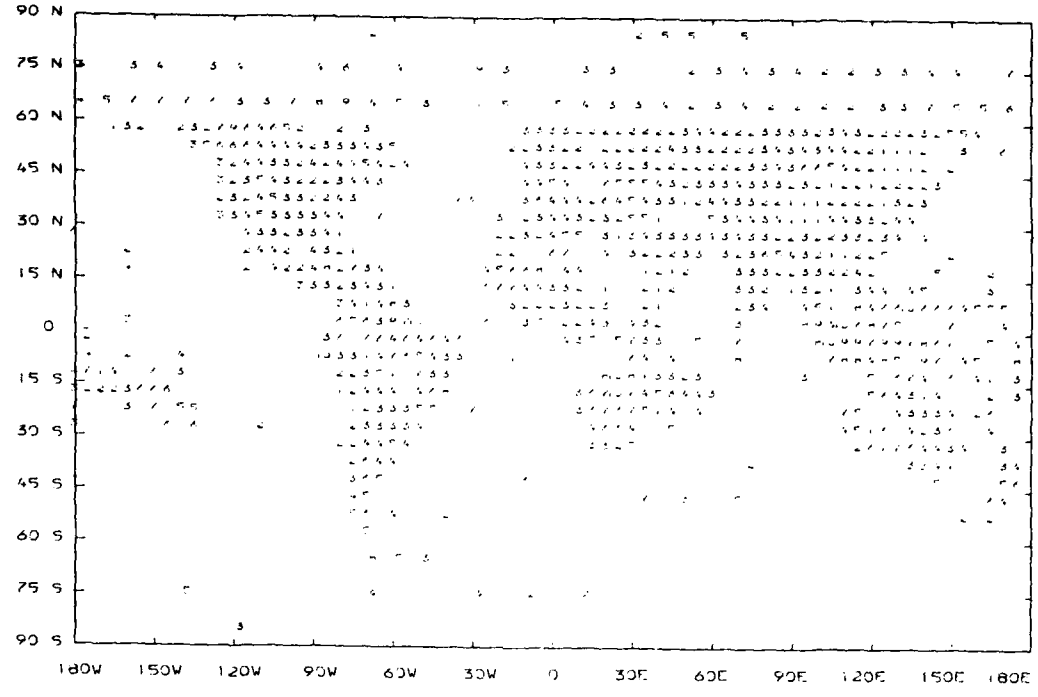

Figure 7 Global distribution of P(U⇒L) for U = Ci/Cs/Cc and L = As/Ac for January 1985

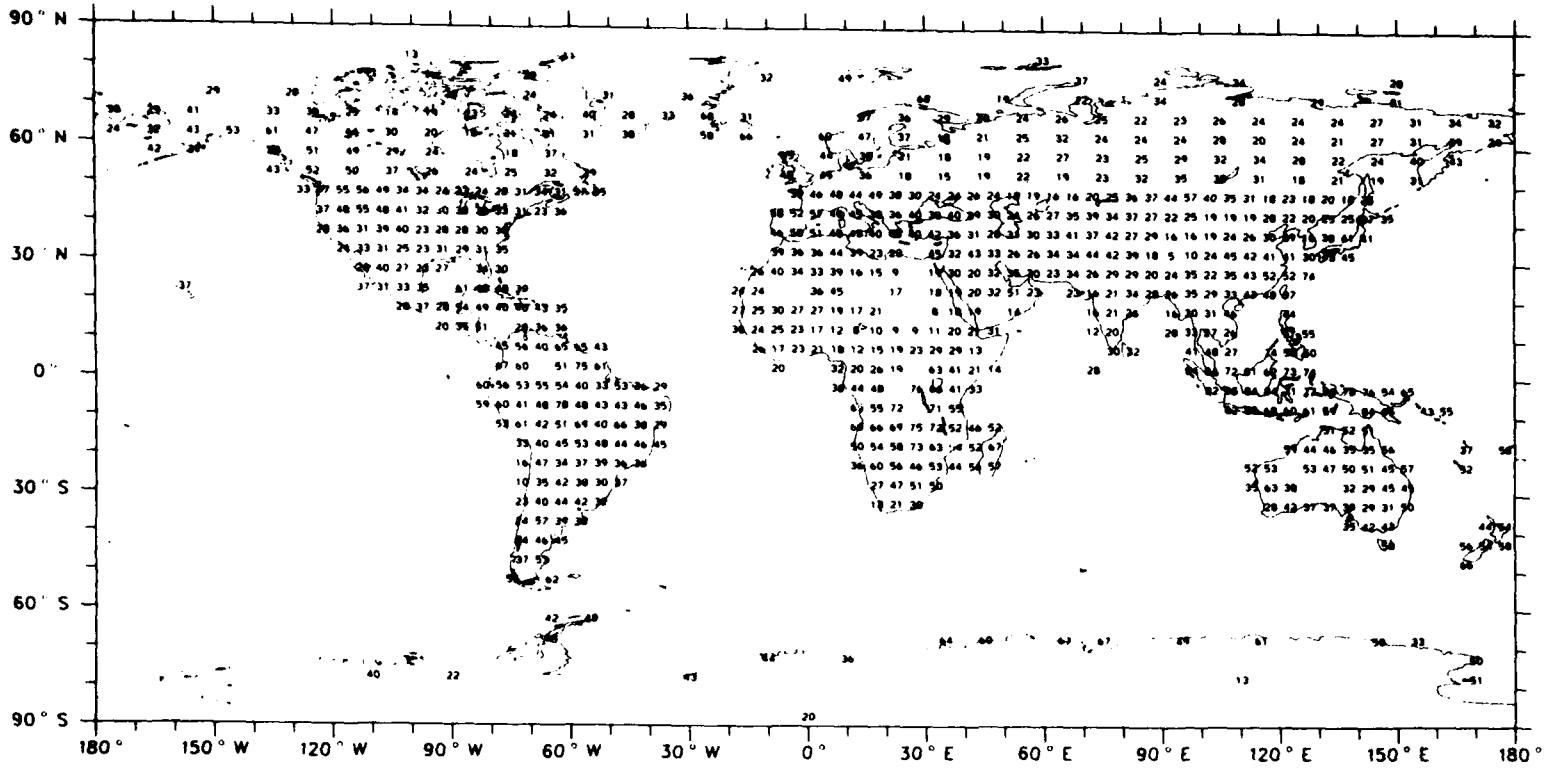

Figure 8 Global distribution of P(U⇒L) for U = Ci/Cs/Cc and L = As/Ac for December, January, February 1971–1980 (from Hahn *et al.*, 1984)

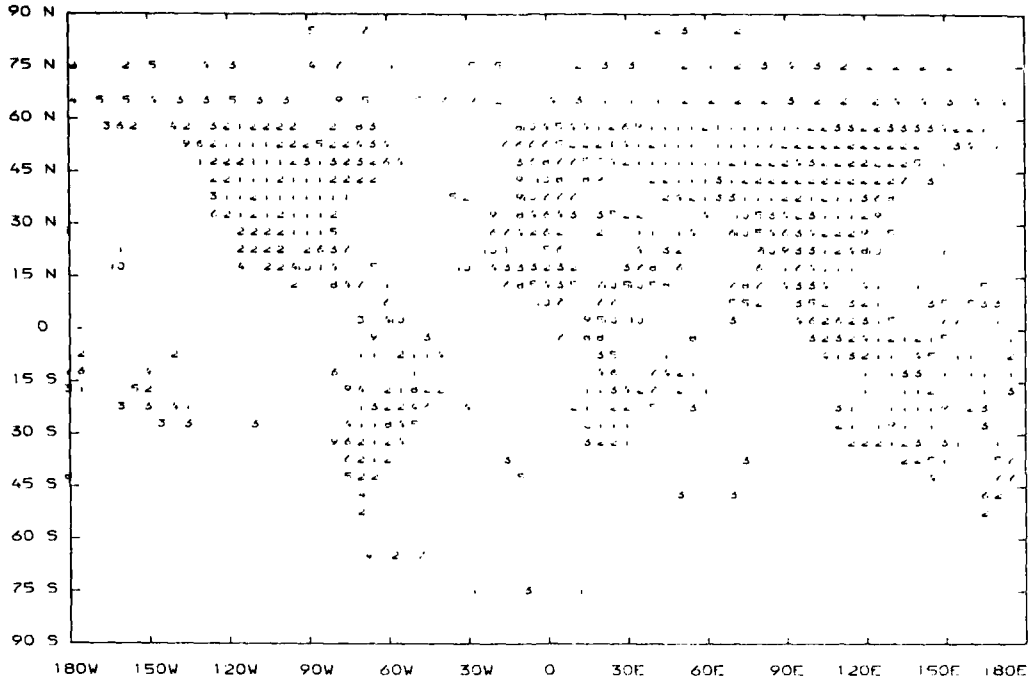

Figure 9 Global distribution of P(U⇒L) for U = Ci/Cs/Cc and L = St/Sc for July 1983

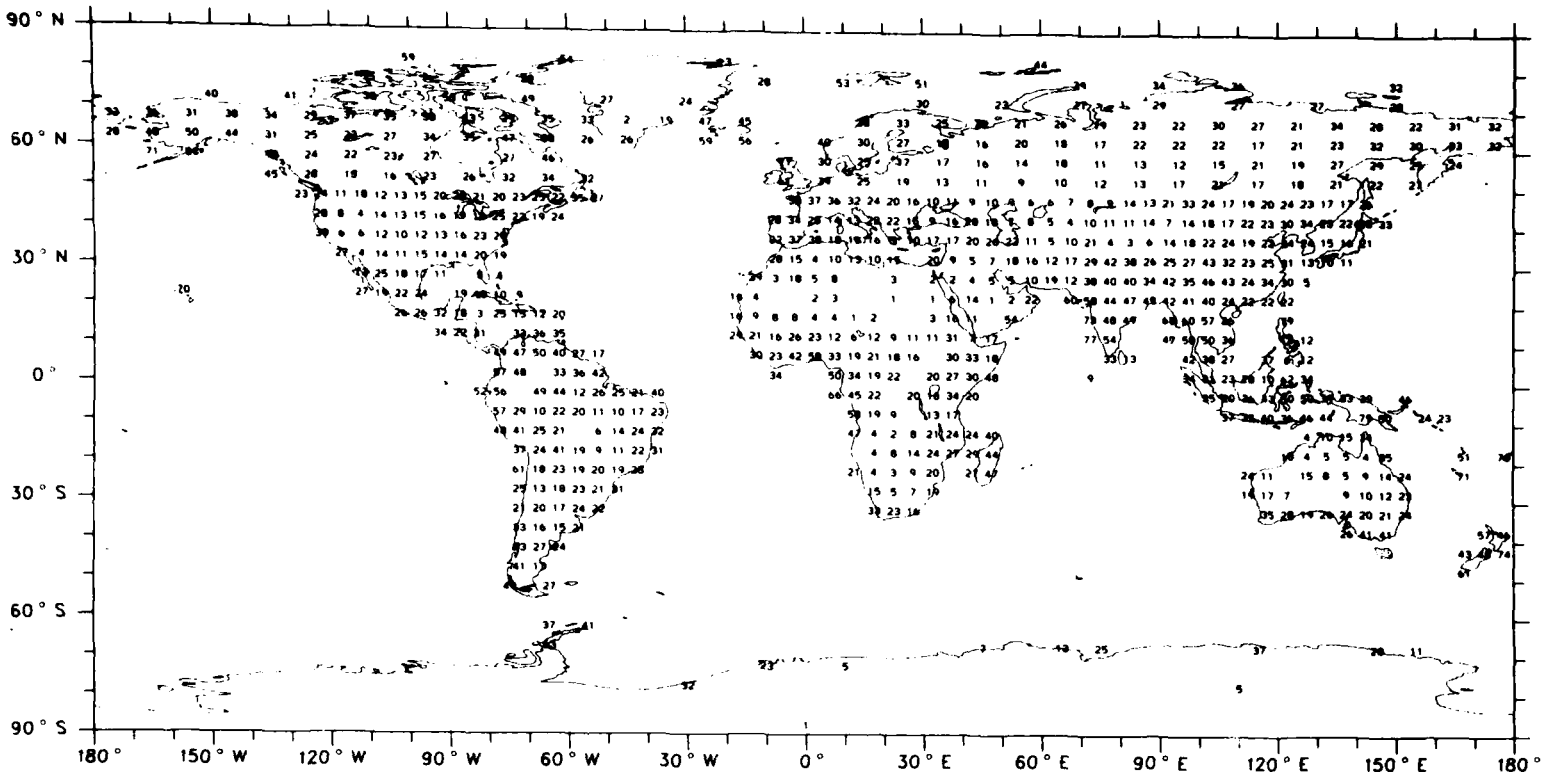

Figure 10 Global distribution of P(U⇒L) for U = Ci/Cs/Cc and L = St/Sc for June, July, August 1971–1980 (from Hahn *et al.*, 1984)

some differences over parts of South America, both patterns correspond well. Amongst the features recognisable in both data sets is the general increase in P(U⇒L) in moving from eastern to western Europe. The monthly map of altiform–stratiform probability provides an example of where short term effects may be influencing the data. Here there is a consistent disagreement around the world with the tendency for the monthly data (especially in July) to give higher values of P(U⇒L) than those of Hahn *et al.*. These differences vary in the range of 10–60% and may be the result of abnormal synoptic patterns during the month. The January monthly result shows rather more agreement where comparison is possible e.g. over central Asia.

Despite, therefore, the rather crude nature of such a comparison it is still of interest to observe how some of the long term characteristics of these maps can be seen in much smaller data samples.

2.5 Overview

Having investigated the behaviour of the P(L⇒U) contingency probability over a data set of comparable or even greater magnitude to that of Hahn *et al.* it has been demonstrated that their assertion that the probability of occurrence of an obscured upper-level cloud is the mean of the probabilities of visible upper-level cloud, though attractive, convenient and with some theoretical backing, does not possess local, regional or global applicability. Values of P(L⇒U) vary with the amount of lower cloud on both hemispheric, regional and particularly local space scales for various cloud type combinations, sometimes to a considerable degree. Due to the relationship between P(L⇒U) and P(U⇒L) and the effect of errors in selection of the appropriate values of the former in estimating the latter, it appears that a careful analysis of the P(L⇒U)/lower cloud amount relationship is advisable in any situation prior to the prediction of P(U⇒L) values.

3. Effects of Temporal Variations in Cloud Amount and Type on the Sea Surface Radiation Budget

3.1 Introduction

The shortwave and longwave components of the radiation budget at the sea surface are known to be a function of cloud amount and type. Accurate estimates of incoming short and longwave radiation are required for radiation budget studies over the ocean and several empirical estimators have been developed to utilise routine surface cloud and other synoptic observations (Lumb, 1964; Kasten and Czeplak, 1979; Lind and Katsaros, 1982). These techniques have been used to predict hourly values of incoming as well as net shortwave and longwave radiation and in comparison with in situ radiance measurements have been shown to be accurate up to ± 10 W m^{-2} over time periods of the order of two weeks.

However, the accuracy of empirical estimators is know to be susceptible to temporal variations in cloud amount and type, particularly in the shortwave region whilst errors in reported cloudiness will induce corresponding errors in both the short and longwave radiation estimates. The objectives in this exercise are to investigate both these effects using routine hourly surface cloud observations and independent high temporal resolution surface cloud observations.

3.2 Data sources

All the data were gathered during the various phases of the Joint Air–Sea Interaction (JASIN) experiment (Pollard, 1978) which took place in the seas located off NW Scotland (Figure 11) in the summer of 1978 and involved intensive in situ field observations with

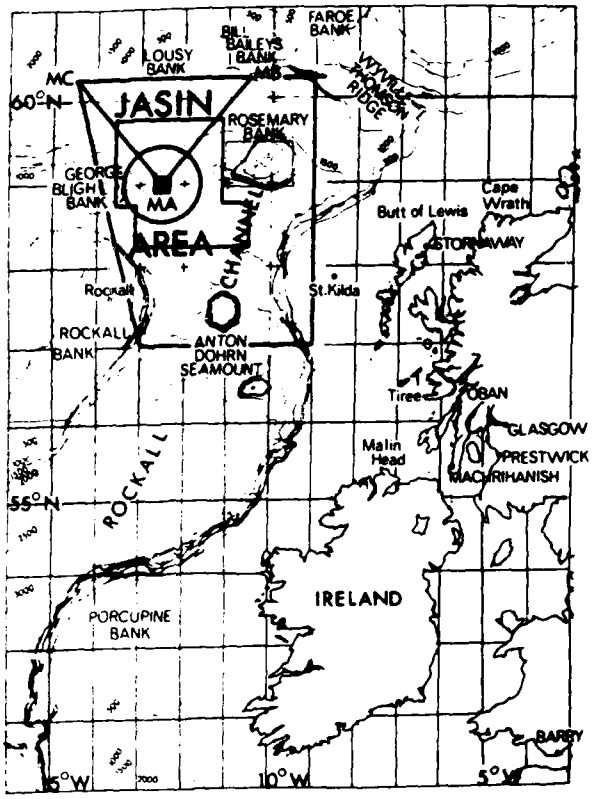

Figure 11 Map showing the location of the JASIN area

the aim of improving the understanding of the atmosphere–ocean interface. Shipboard cloud and radiation observations were recorded aboard HMS Hecla stationed at 60°15' N, 14°30' W. Routine hourly synoptic meteorological observations included information on total cloud amount and on individual cloud layers present. On certain selected days and times (listed in Table 1) an all sky camera was also operated on board recording the cloud cover at five minute intervals. Appropriate instrumentation (see Lind *et al.*, 1984) was set up to measure each incoming component of the radiation budget.

3.3 Analysis of cloud images

The all-sky cloud images were analysed separately for (i) total, (ii) high cloud amount by projecting each image on to the equidistant grid shown in Figure 12 and treating each grid portion separately. The cumulative okta count for all 34 grid segments is then divided by 272 to obtain the overall total or high cloud amount in an image.

Since these estimates will be used in radiation computations, it was important to obtain an independent analysis of a sample of the images to check on the accuracy of observation. A 10% sample containing some of the more 'difficult' clouds was selected and analysed separately by Anthony Andrews (AA). The sample was taken from four different days (August 20th, 22nd, 25th and September 2nd) and the results of the original intercomparison of his and the retrievals by AG is shown in Figures 13 to 20 inclusive. These intercomparisons are important in evaluating any significant bias in either total or high cloud amount that may be affecting the long term quality of the AG retrievals. For example, if it was discovered that in the 10% sample there was a consistent relative overestimate of total cloud amount in the order of 15% by AG, confirmed after reanalysis, this would have to be carried over into the comparison with the conventional reports.

Table 1 Dates and times of the JASIN all-sky images selected for analysis

Month	*Date*	*Time Periods of Images*	
July 1978	20	0735–1150	
	21	0925–1755	
	22	0940–1115	1315–1800
	24	0610–1620	
	25	0340–1245	1330–1800
	26	0750–0900	1500–2030
August 1978	20	0730–1300	
	22	0720–1400	1400–1950
	23	0600–0940	1115–2015
	24	0600–1245	1320–2115
	25	0600–1300	1310–2000
	29	0700–1350	1505–2000
	30	0615–1315	
	30	0720–1340	
September 1978	1	0600–1240	1250–1930
	2	0600–1250	1250–1950
	3	0645–0720	
	4	0720–1420	
	5	0600–0715	

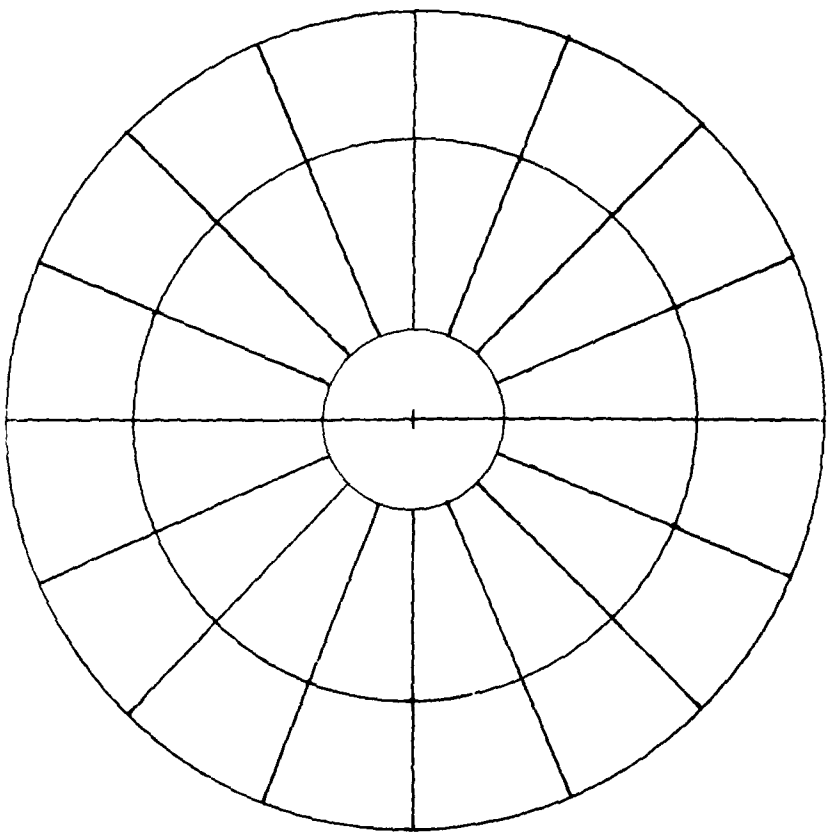

FIgure 12 Grid used in all-sky camera cloud amount retrievals

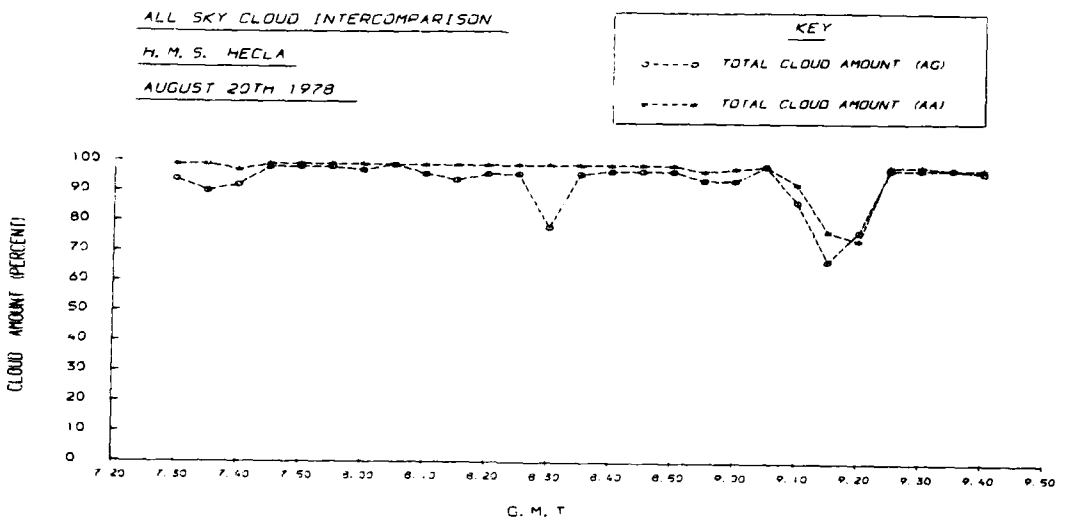

Figure 13 All sky cloud retrieval intercomparison of total cloud amount for August 20th 1978

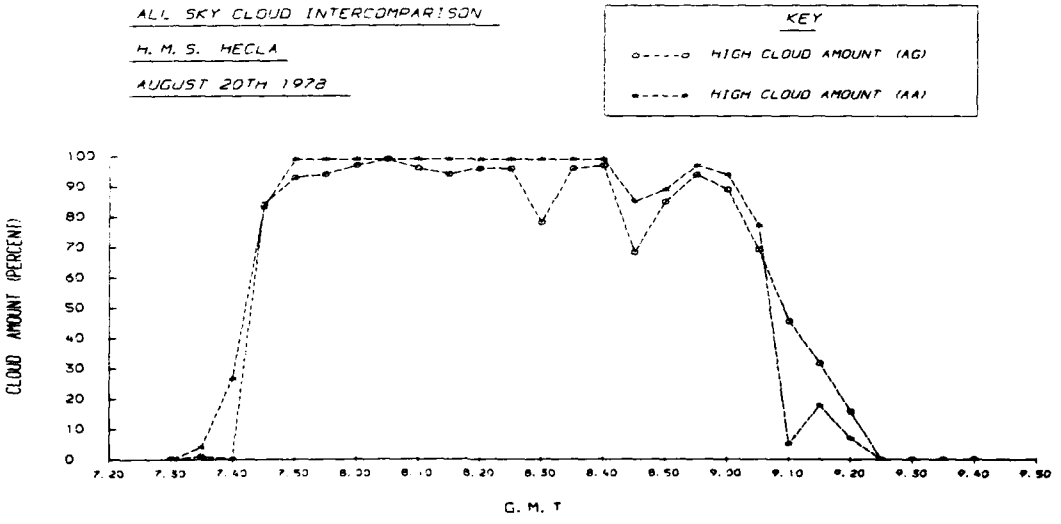

Figure 14 All sky cloud retrieval intercomparison of high cloud amount for August 20th 1978

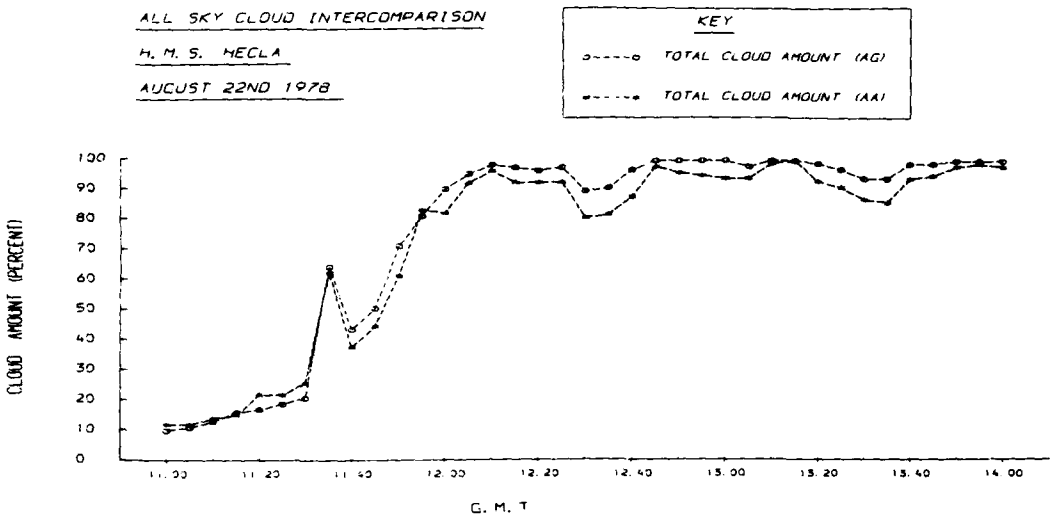

Figure 15 All sky cloud retrieval intercomparison of total cloud amount for August 22nd 1978

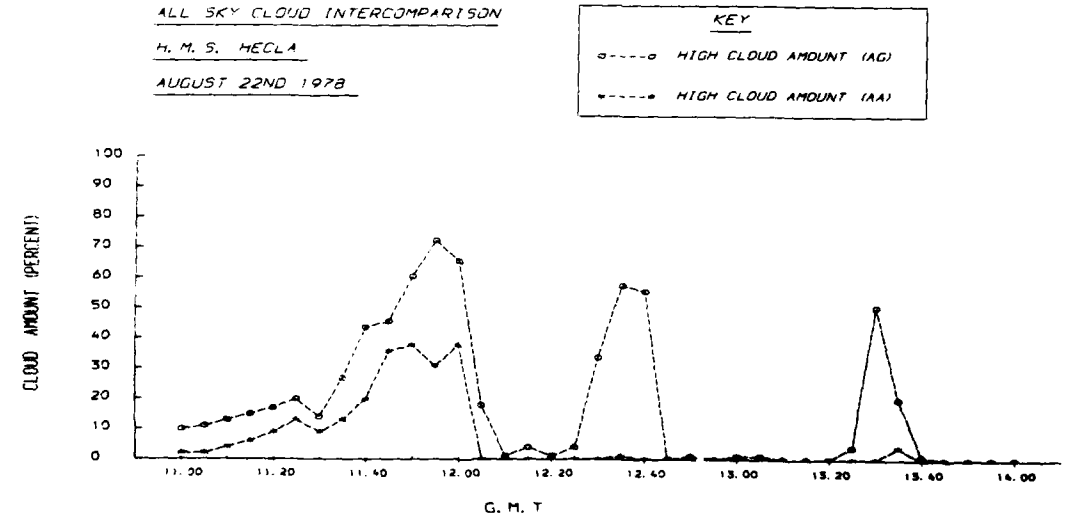

Figure 16 All sky cloud retrieval intercomparison of high cloud amount for August 22nd 1978

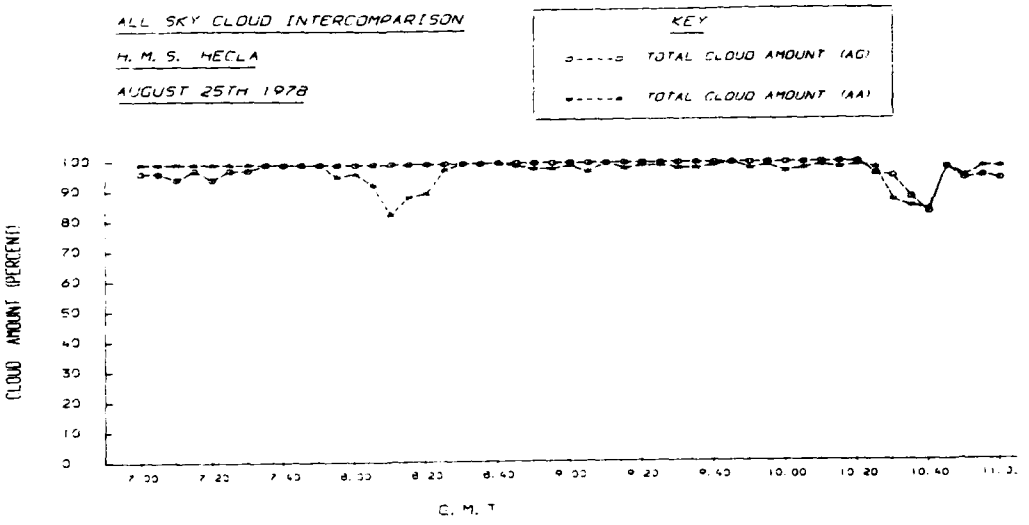

Figure 17 All sky cloud retrieval intercomparison of total cloud amount for August 25th 1978

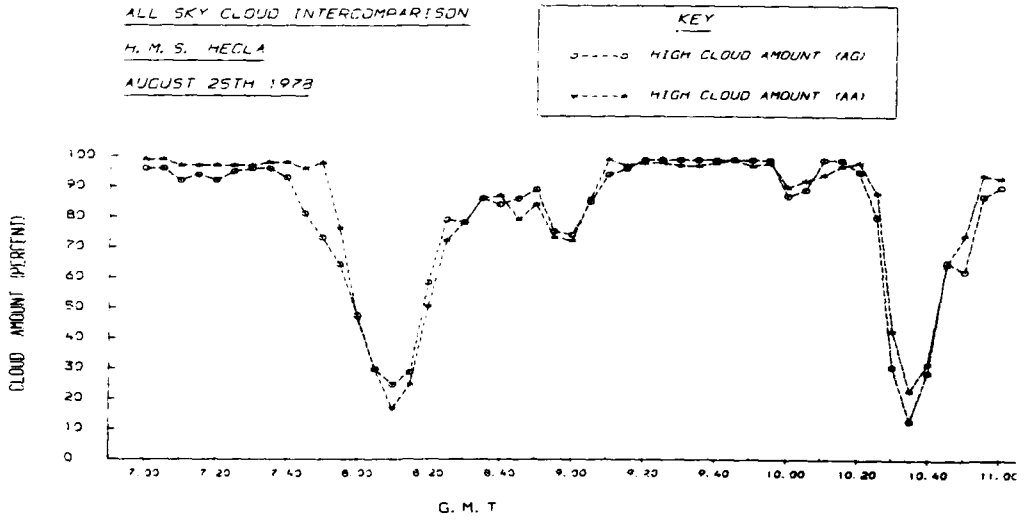

Figure 18 All sky cloud retrieval intercomparison of high cloud amount for August 25th 1978

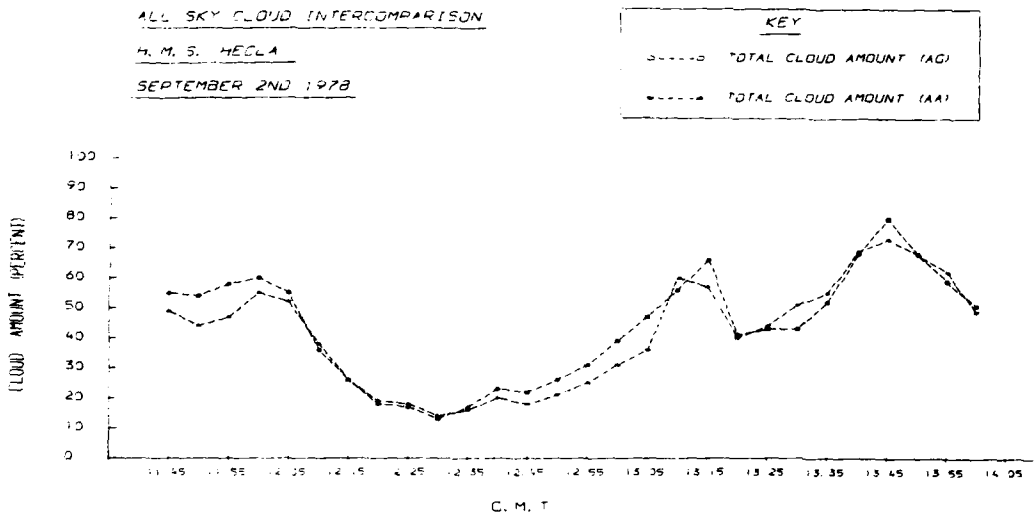

Figure 19 All-sky cloud retrieval intercomparison of total cloud amount for September 2nd 1978

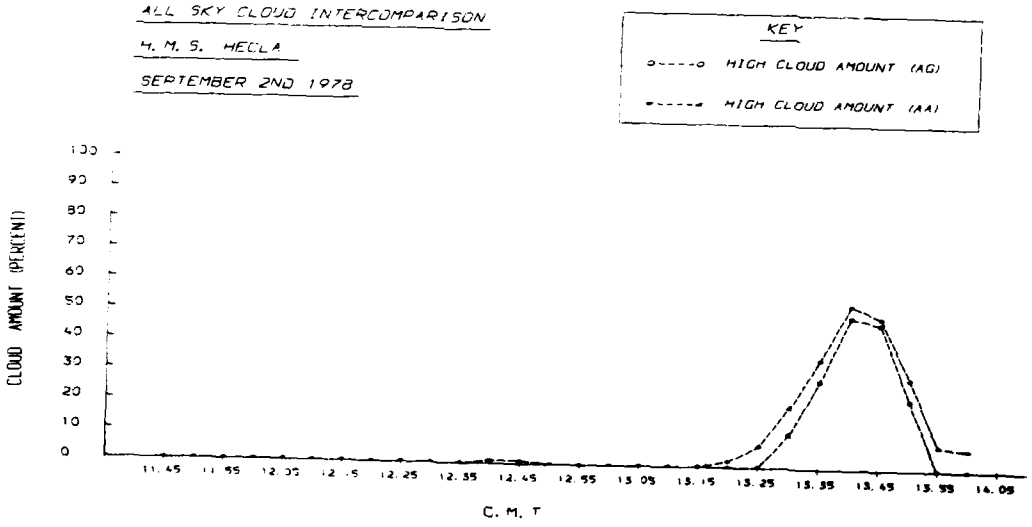

Figure 20 All-sky cloud retrieval intercomparison of high cloud amount for September 2nd 1978

In fact, Figures 13–20 reveal fairly consistent agreement between the two independent analyses with one particular exception. This was the discrepancy in high cloud amount on 22nd August (Figure 16). The set of images from that day were reanalysed by AG with an almost identical result being obtained. Significantly, the presence of high cloud during the time periods 12.25 to 12.40 and 13.25 to 13.35 was also confirmed. Overall there was judged to be no predominant bias either way in the AG retrievals on the basis of these results.

3.4 Comparison of all-sky camera and conventional observations

The all-sky camera analyses were then plotted against the observations made from the bridge of H.M.S. Hecla. Figures 21 to 37 depict the day by day comparison of total for each of the 17 days listed in Table 1 whilst Figures 38 to 45 show the corresponding results for high cloud. These are fewer in number due to the fewer days on which significant amounts of high cloud were reported by the bridge or observed by the all-sky camera. On the total cloud diagrams the absolute difference between bridge and camera is marked with a cross.

The first half of the analysis period was dominated by large amounts of stratiform cloud whilst in the second half the cloud cover tended to be more broken with cumulus and, particularly, cirrus present. It can be seen that discrepancies between the two types of report are widespread and occasionally in excess of 4 oktas, especially for high cloud. There were some instances of differences arising when the camera image clearly indicated an overcast sky whilst the bridge report was contradictory. It was decided to diagnose all errors in excess of one okta remembering that:

i) The all-sky camera provides a much more deliberate and precise method of analysis and

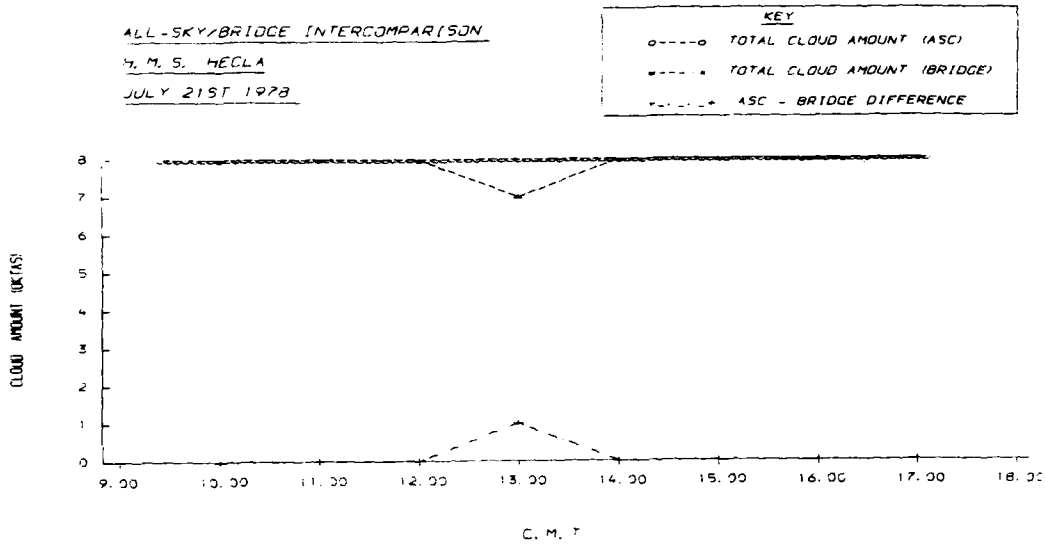

Figure 22 All-sky/bridge total cloud intercomparison for July 21st 1978

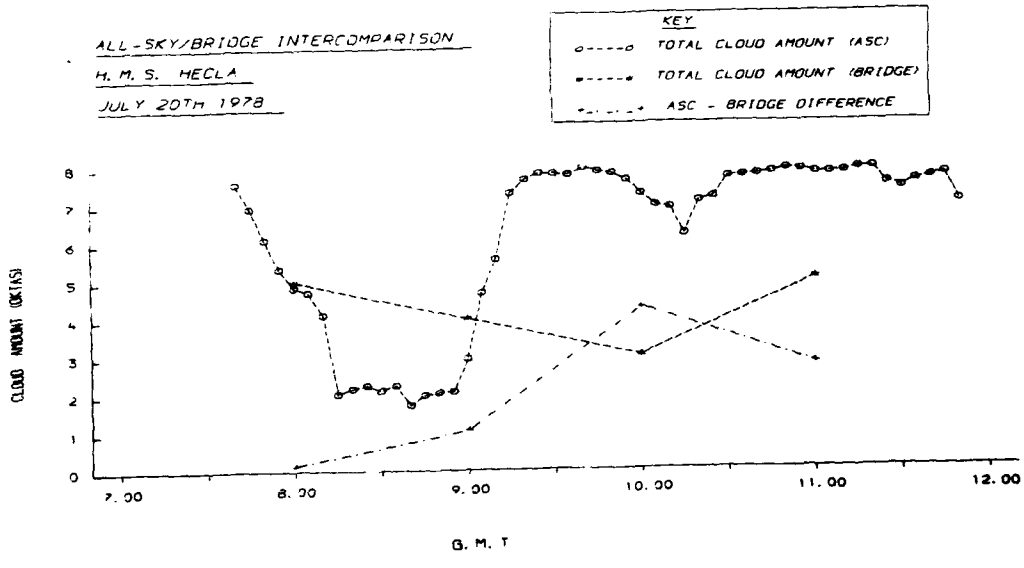

Figure 21 All-sky/bridge total cloud intercomparison for July 20th 1978

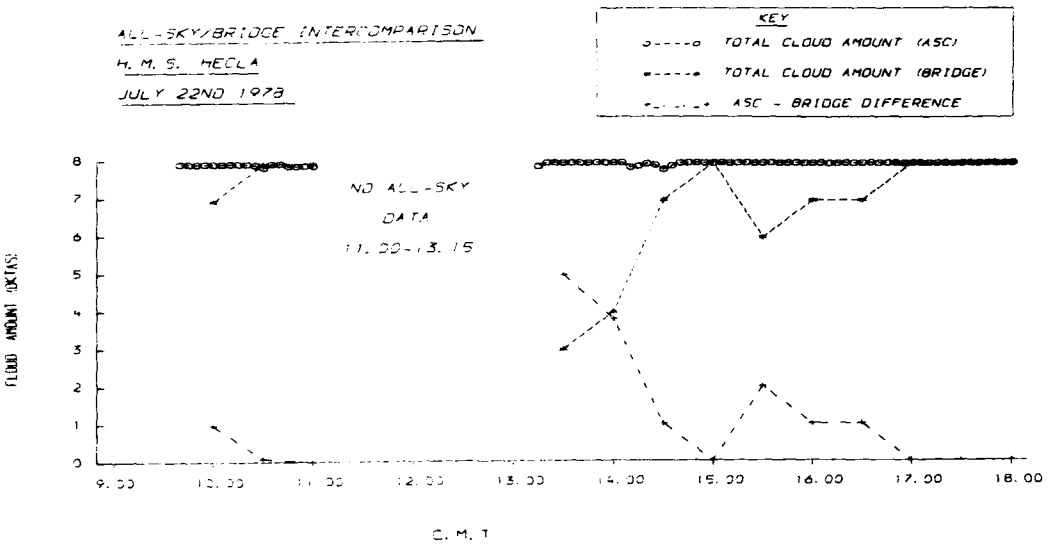

Figure 23 All-sky/bridge total cloud intercomparison for July 22nd 1978

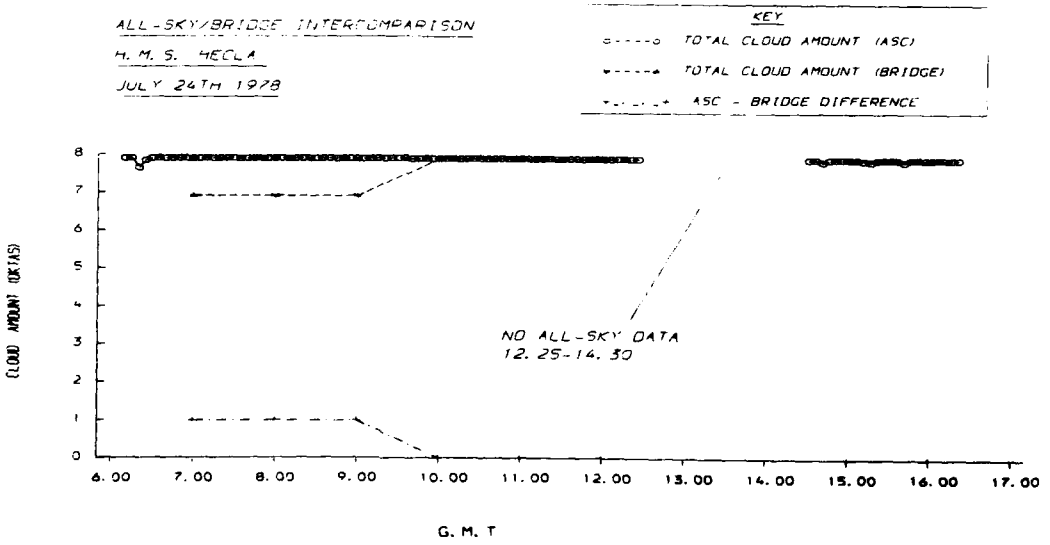

Figure 24 All-sky/bridge total cloud intercomparison for July 24th 1978

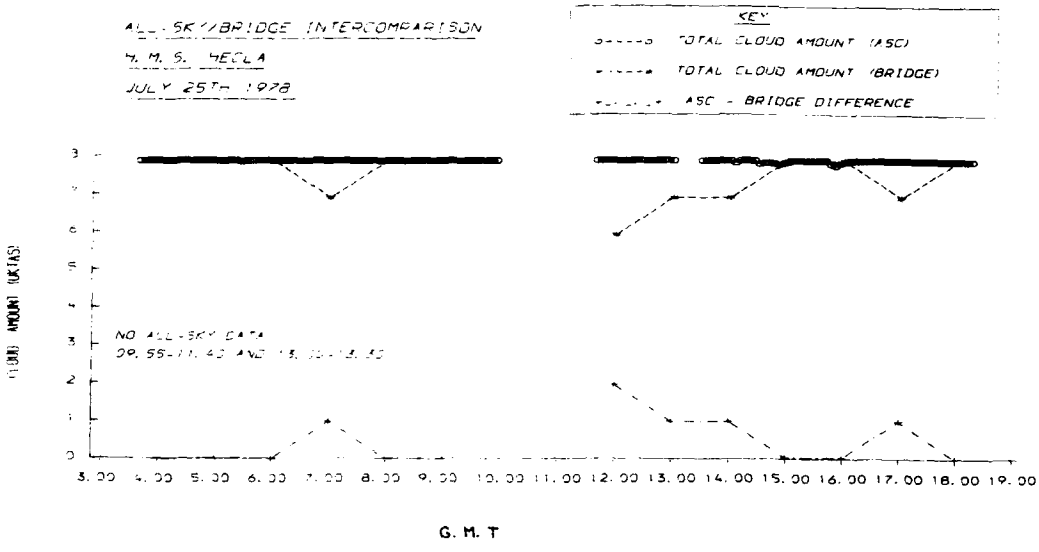

Figure 25 All-sky/bridge total cloud intercomparison for July 25th 1978

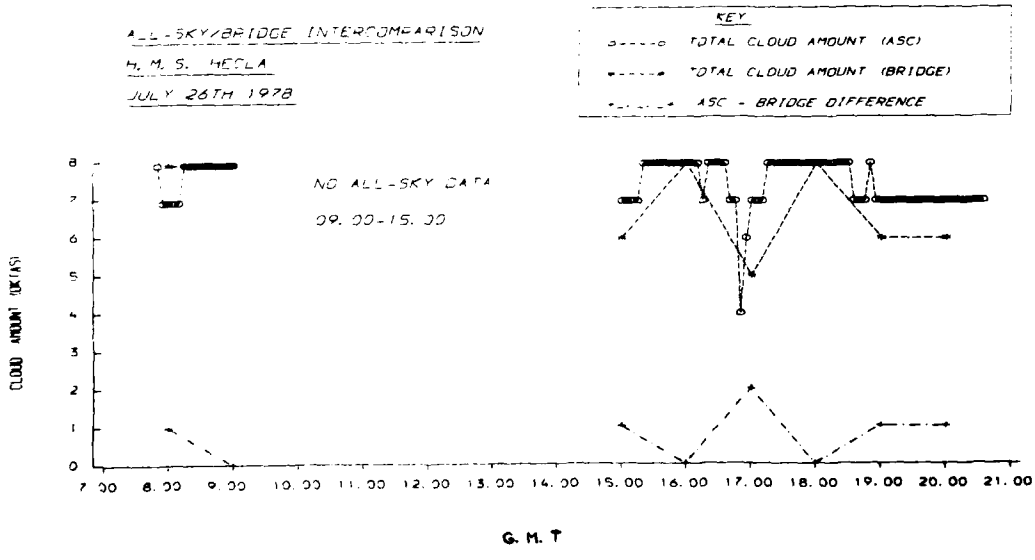

Figure 26 All-sky/bridge total cloud intercomparison for July 26th 1978

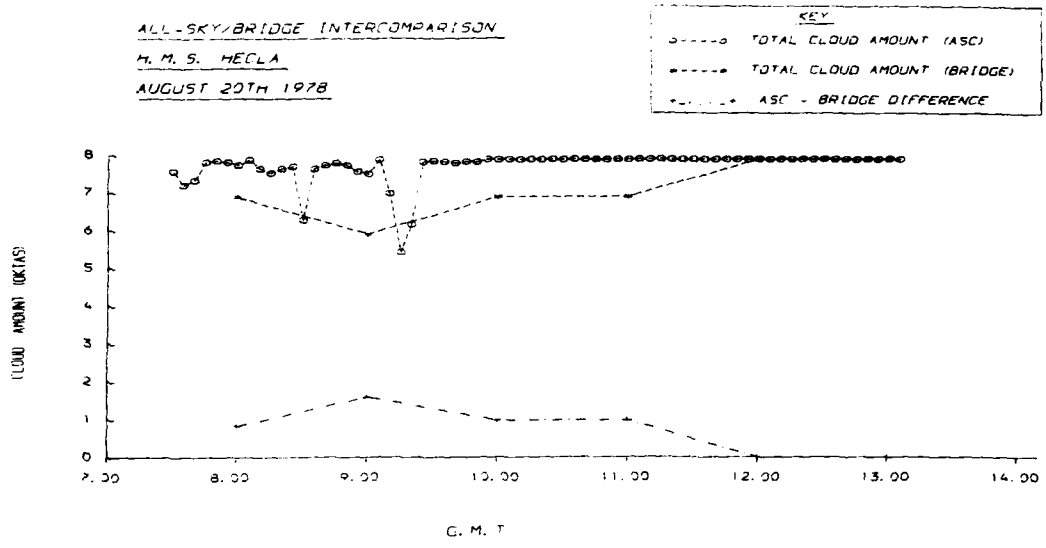

Figure 27 All-sky/bridge total cloud intercomparison for August 20th 1978

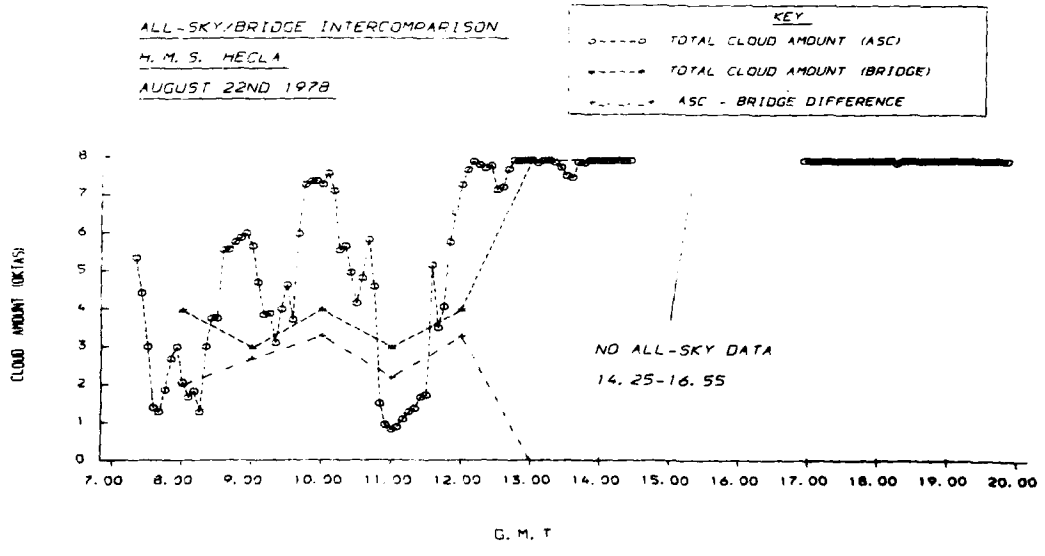

Figure 28 All-sky/bridge total cloud intercomparison for August 22nd 1978

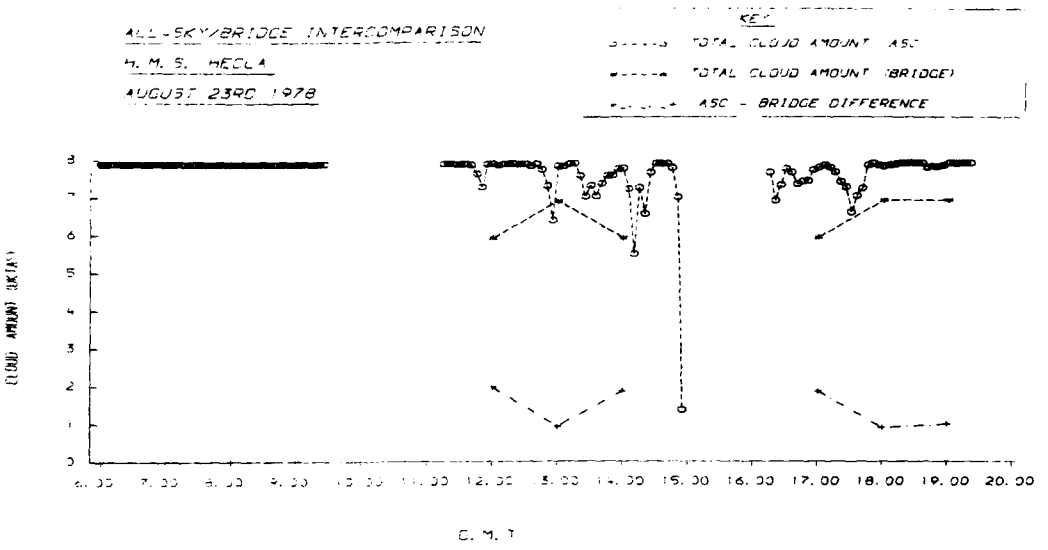

Figure 29 All-sky/bridge total cloud intercomparison for August 23rd 1978

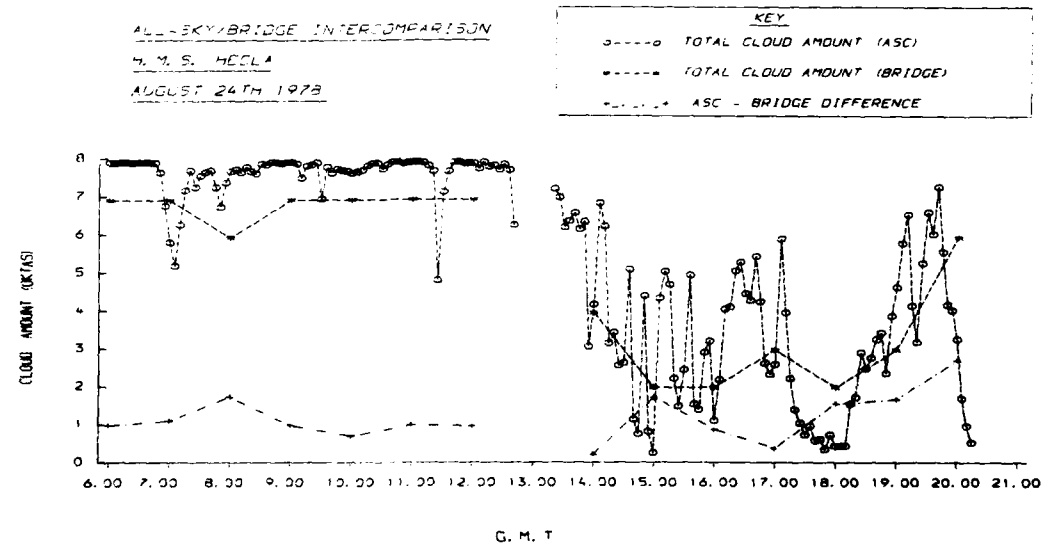

Figure 30 All-sky/bridge total cloud intercomparison for August 24th 1978

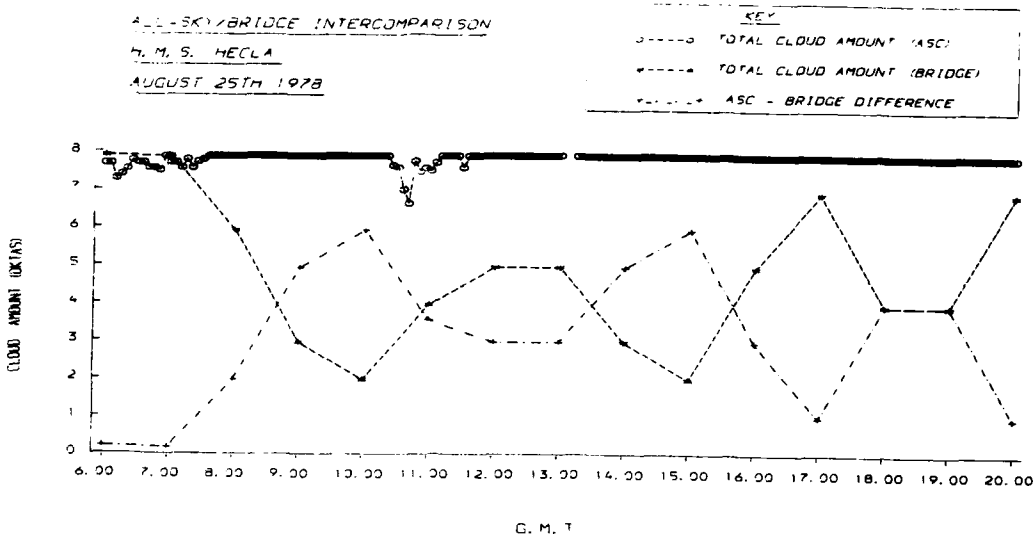

Figure 31 All-sky/bridge total cloud intercomparison for August 25th 1978

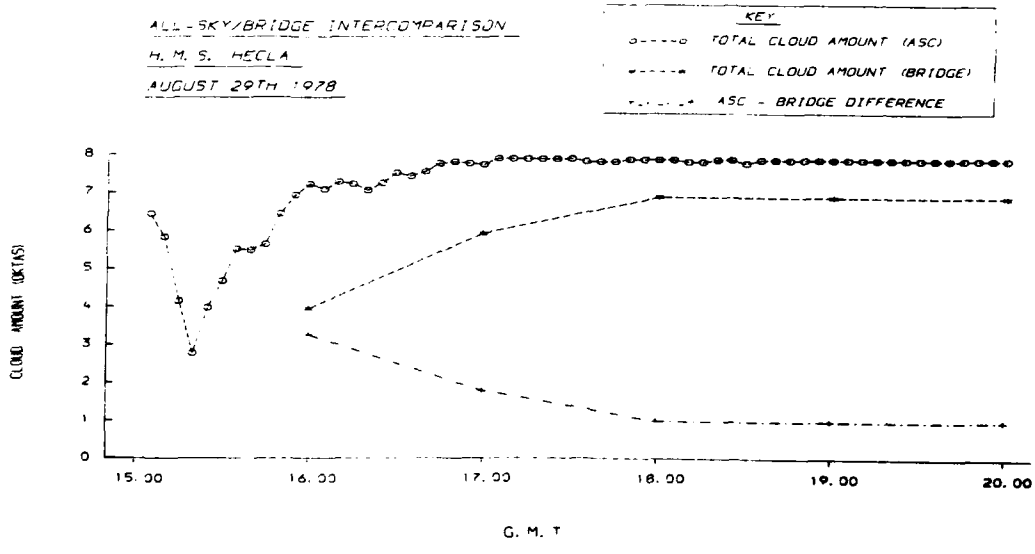

Figure 32 All-sky/bridge total cloud intercomparison for August 29th 1978

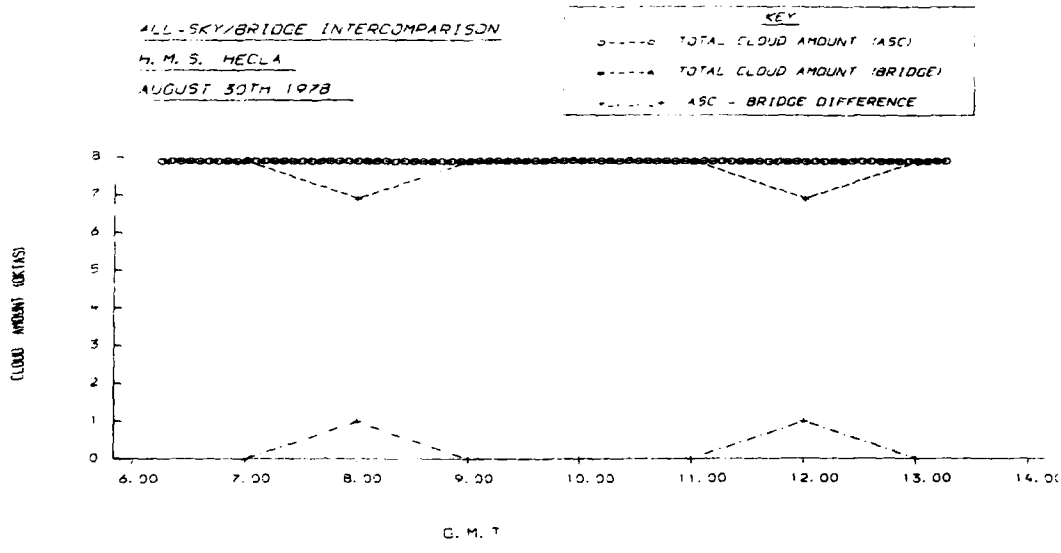

Figure 33 All-sky/bridge total cloud intercomparison for August 30th 1978

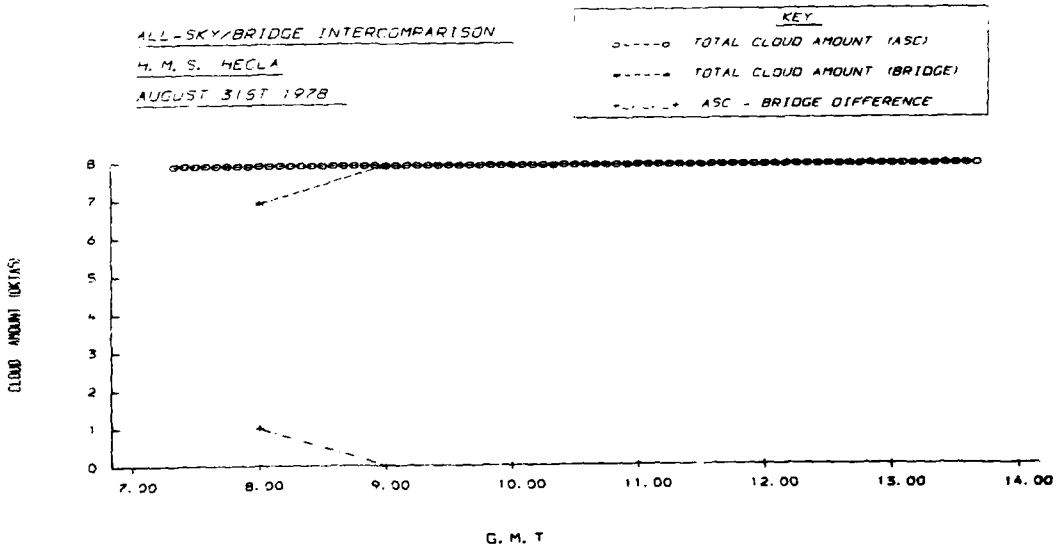

Figure 34 All-sky/bridge total cloud intercomparison for August 31st 1978

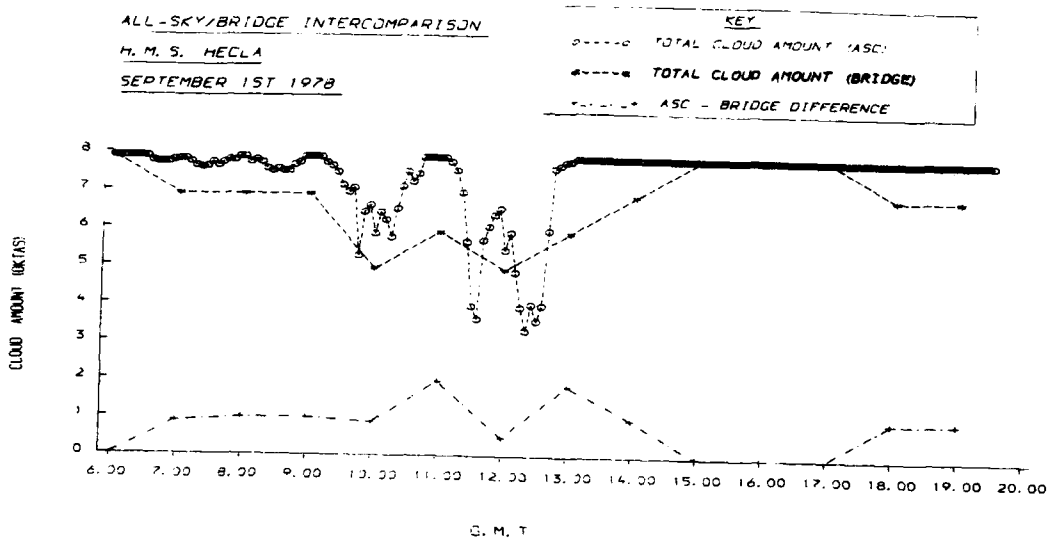

Figure 35 All-sky/bridge total cloud intercomparison for September 1st 1978

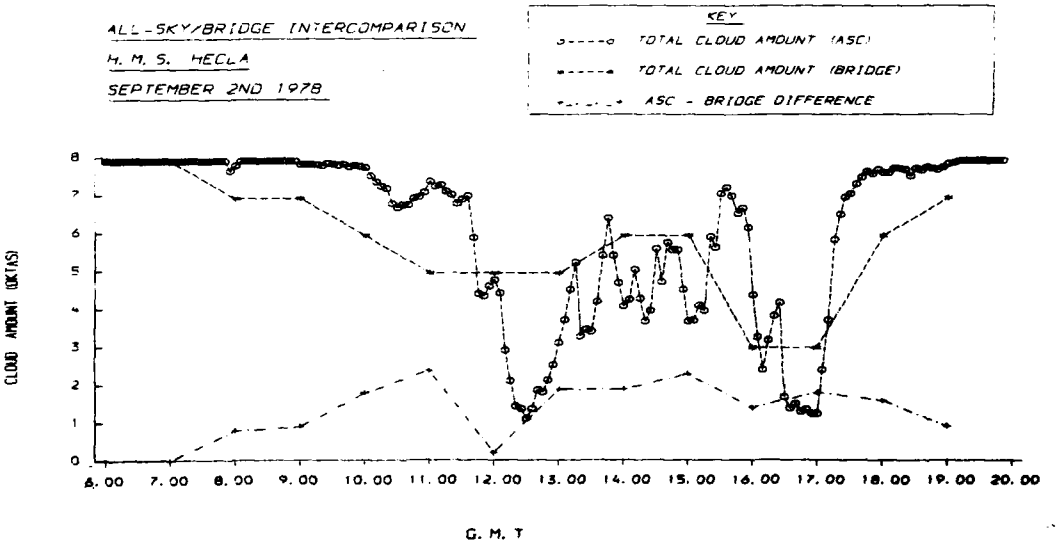

Figure 36 All-sky/bridge total cloud intercomparison for September 2nd 1978

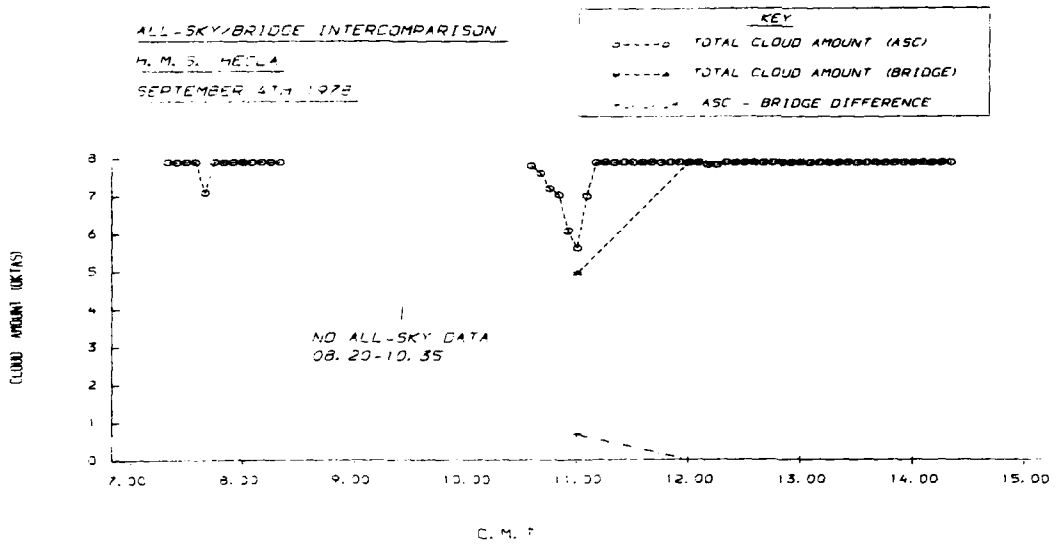

Figure 37 All-sky/bridge total cloud intercomparison for September 4th 1978

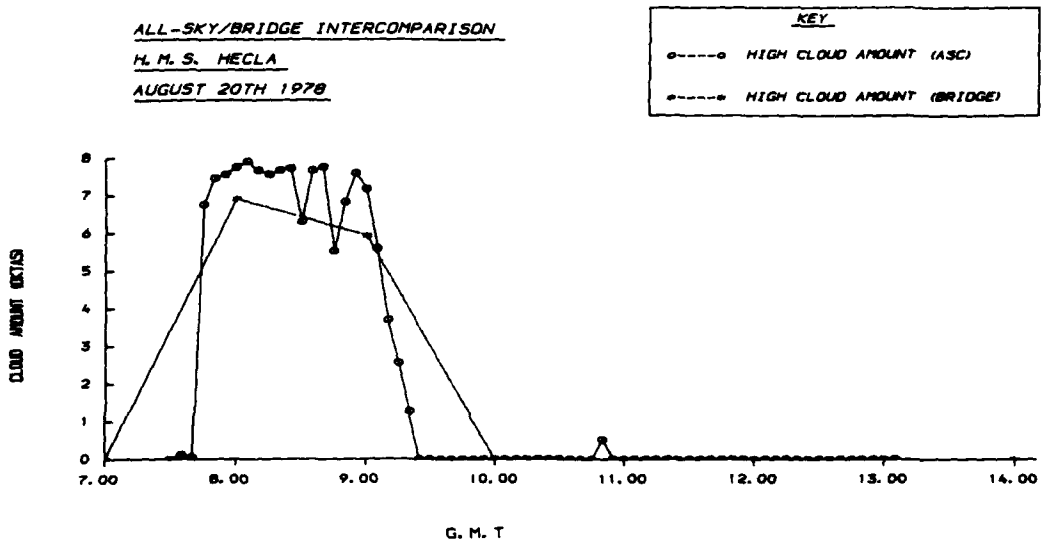

Figure 38 All-sky/bridge high cloud intercomparison for August 20th 1978

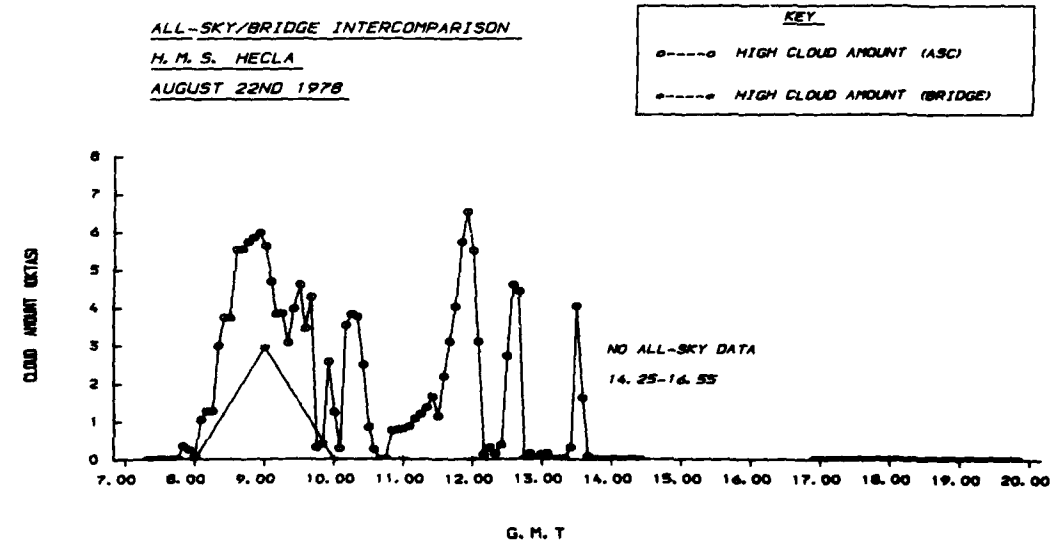

Figure 39 All-sky/bridge high cloud intercomparison for August 22nd 1978

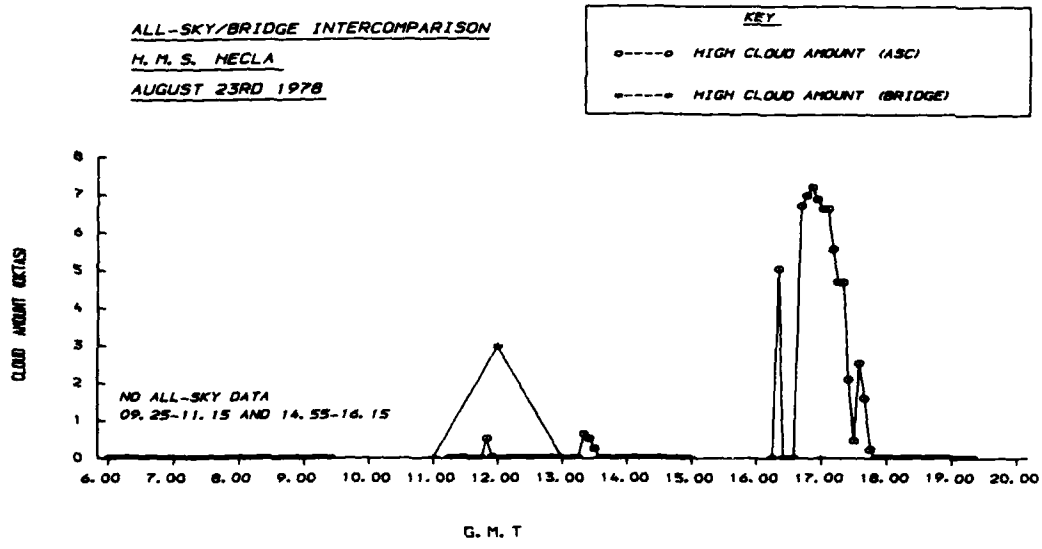

Figure 40 All-sky/bridge high cloud intercomparison for August 23rd 1978

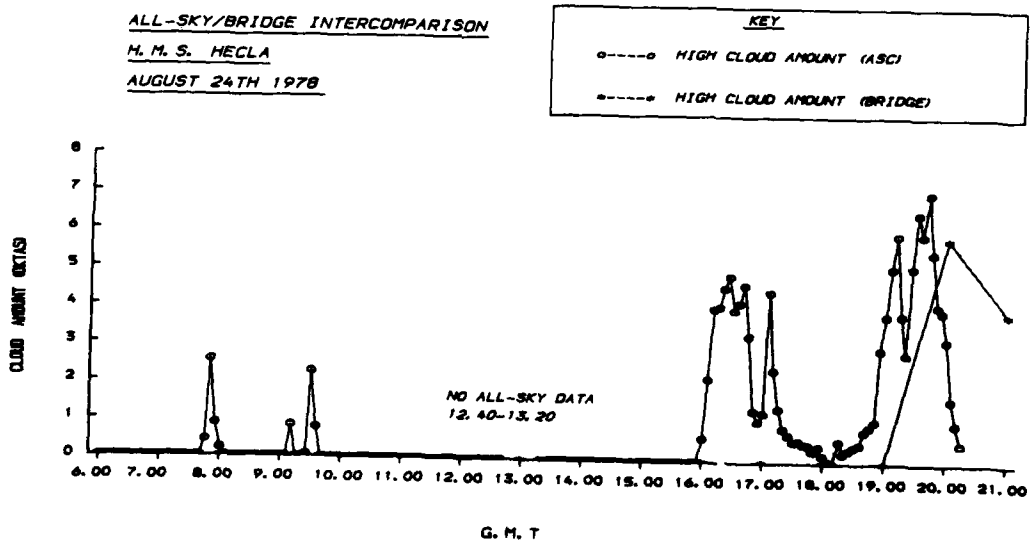

Figure 41 All-sky/bridge high cloud intercomparison for August 24th 1978

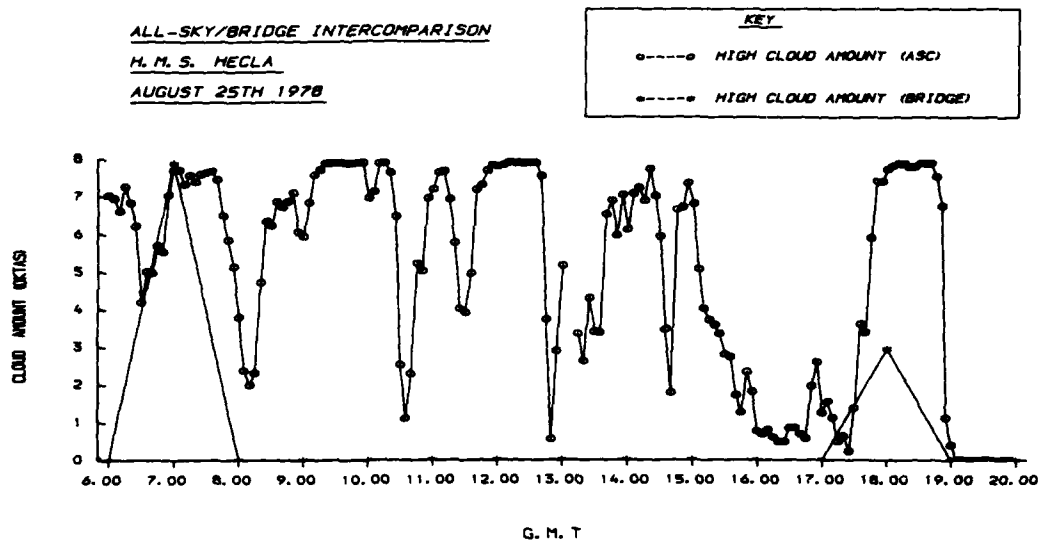

Figure 42 All-sky/bridge high cloud intercomparison for August 25th 1978

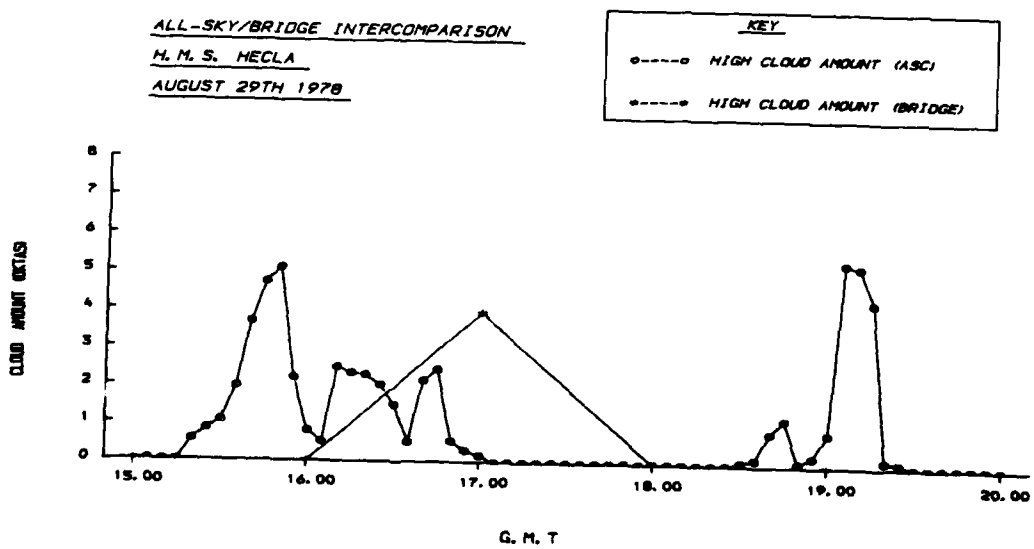

Figure 43 All-sky/bridge high cloud intercomparison for August 29th 1978

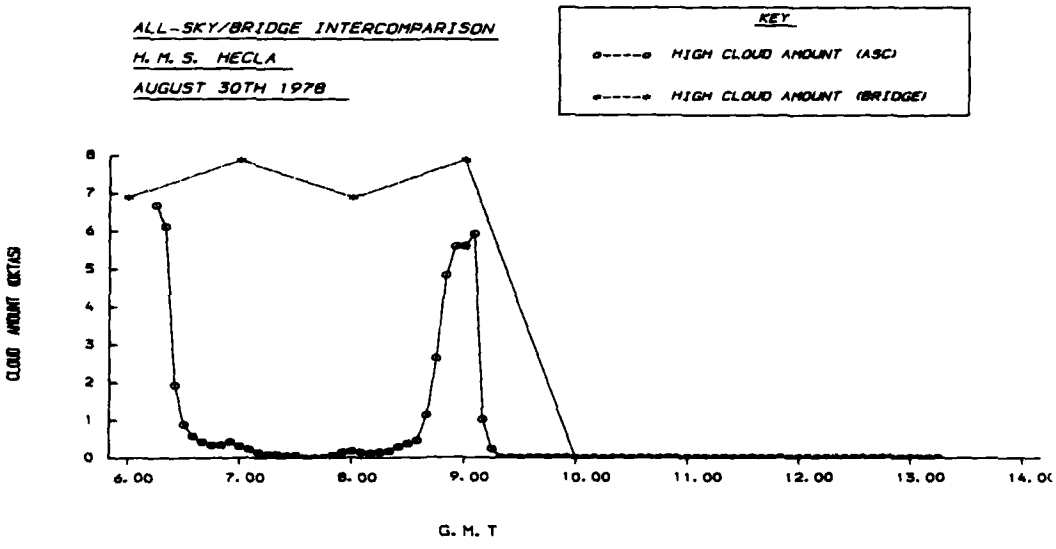

Figure 44 All-sky/bridge high cloud intercomparison for August 30th 1978

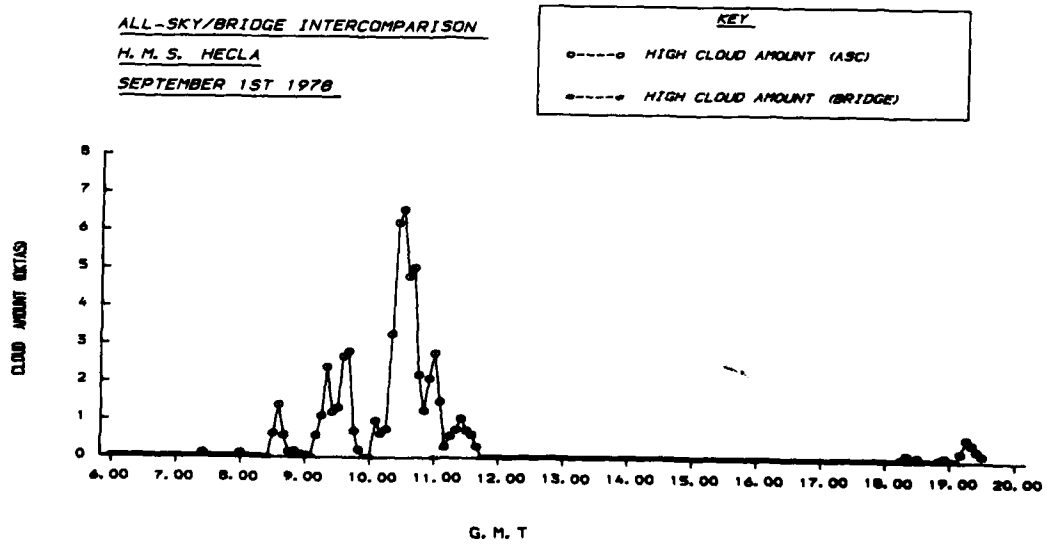

Figure 45 All-sky/bridge high cloud intercomparison for September 1st 1978

ii) The bridge reports are made to the nearest okta. The exercise revealed that in many cases the difference in estimates was due to the tendency for the bridge observer to either i) incorrectly estimate the cloud amount to the nearest okta or ii) fail to report the presence of high cloud, particularly the thin, semitransparent high cloud that does not always assume a well-recognised form, and thus highlighted the potential values of all-sky retrievals in modifying poor conventional reports. Table 2 lists the times, differences and probable causes discovered.

The latter half of the selected JASIN days provided examples of rapid changes of cloud amount on time scales of less than one hour. The periods between 15.00 and 16.00 hours on 24th August (Figure 30) and between 12.00 and 13.00 hours on 2nd September (Figure 36) are cases in question. In such situations the high variability in cloudiness can render hourly estimates unrepresentative of the intervening period, especially if the amount of cloud in that period has been consistently biased high or low with respect to the hourly report. This can have serious implications in shortwave radiation calculations. In order to assess how representative hourly reports actually are of the surrounding time the all-sky data from four days which experienced some of the more variable cloud cover were used to calculate hourly means of total cloudiness centred on the hourly bridge report times. These were set against i) hourly all-sky data and ii) the hourly bridge data. The results are given in Figures 46 to 49 which show maximum differences of the order of two and a half oktas with generally larger differences in comparison with the bridge observations due to their frequent departure from the hourly all-sky retrievals.

Table 2 Times and diagnosis of camera/bridge cloud amount differences

Date	Time	Difference (Oktas)	Cloud Type Total(T) or High(H)	Camera(C) or Bridge(B) relative overestimate	Suggested Diagnosis
July 20th	10.00	4.3	(T)	C	Bridge underestimate
July 20th	11.00	3.0	(T)	C	Bridge underestimate
July 22nd	13.30	5.0	(T)	C	Definite Overcast, Bridge underestimate
July 22nd	14.00	3.8	(T)	C	Definite Overcast, Bridge underestimate
July 22nd	15.30	2.0	(T)	C	Definite Overcast, Bridge underestimate
July 25th	12.00	2.0	(T)	C	Definite overcast, bridge underestimate
July 26th	17.00	3.0	(T)	C	Bridge underestimate, maybe due to poor synchronization
August 22nd	8.00	2.0	(T)	B	Bridge overestimate
August 22nd	9.00	2.6	(H)	C	Bridge underestimate of thin cirrus boundary
August 22nd	10.00	3.0	(T,H)	C	Bridge underestimate of altocumulus, cirrus undetected by bridge
August 22nd	11.00	2.0	(H)	B	Cirrus misinterpreted and overestimate by bridge
August 22nd	12.00	3.0	(T,H)	C	Altocumulus underestimated by bridge, obvious cirrus not reported by bridge
August 23rd	12.00	2.0	(T)	C	Definite overcast, bridge error
August 23rd	14.00	2.0	(T)	C	Bridge underestimate, possibly due to poor timing
August 23rd	17.00	2.0	(T,H)	C	Small gaps overestimated by bridge, high not reported either

Table 2 continued

Date	Time	Difference (Oktas)	Cloud Type Total(T) or High(H)	Camera(C) or Bridge(B) relative overestimate	Suggested Diagnosis
August 24th	8.00	1.9	(T)	C	Bridge overestimate of size of gaps
August 24th	15.00	1.9	(T)	B	Very little cloud, bridge overestimate
August 24th	18.00	1.8	(T,H)	B	Bridge overestimating cumulus
August 24th	19.00	1.9	(H)	C	High not reported by bridge
August 24th	20.00	2.4	(H)	B	Overestimate of cirrus by bridge
August 25th	8.00	2.0	(H)	C	Thin high cloud missed by bridge
August 25th	9.00	5.0	(H)	C	All thin cirrus not reported by bridge
August 25th	10.00	6.0	(H)	C	Thin cirrus missed by bridge
August 25th	11.00	3.6	(H)	C	Obvious cirrus not reported by bridge
August 25th	12.00	3.0	(H)	C	Thin cirrus missed by bridge — possible miscoding
August 25th	13.00	3.0	(T,H)	C	Stratocumulus overestimated slightly by bridge but not thin cirrus reported
August 25th	14.00	5.0	(H)	C	Possible misinterpretation by camera analyst
August 25th	15.00	6.0	(H)	C	Very thin high cloud not reported by bridge
August 25th	16.00	3.0	(T)	C	Bridge underestimate
August 25th	18.00	4.0	(H)	C	Thin high cloud not reported by bridge
August 25th	19.00	5.0	(T)	C	Almost overcast — bridge error

Table 2 continued

Date	Time	Difference (Oktas)	Cloud Type Total(T) or High(H)	Camera(C) or Bridge(B) relative overestimate	Suggested Diagnosis
August 29th	16.00	3.2	(T,H)	C	Cirrus not reported by bridge, camera analyst may have overestimated total
August 29th	17.00	1.8	(T,H)	C	Bridge has overestimated cirrus but largely underestimate to
September 1st	11.00	2.0	(H)	C	Thin cirrus undetected by bridge
September 1st	13.00	2.0	(T)	C	Definite overcast, bridge underestimate
September 2nd	10.00	1.9	(T)	C	Bridge overestimated size of gap near horizon
September 2nd	11.00	2.3	(T)	C	Bridge underestimate of altocumulus
September 2nd	13.00	1.9	(T)	B	Bridge overestimate of altocumulus
September 2nd	14.00	1.9	(T)	B	Bridge overestimate of altocumulus
September 2nd	15.00	2.1	(T)	B	Bridge overestimate
September 2nd	16.00	1.5	(T)	C	Bridge overestimating zenith gap betwen cumulus
September 2nd	17.00	1.7	(T)	B	Bridge overestimating cloud near horizon
September 2nd	18.00	1.5	(T)	C	Bridge underestimate of stratiform/altiform cloud

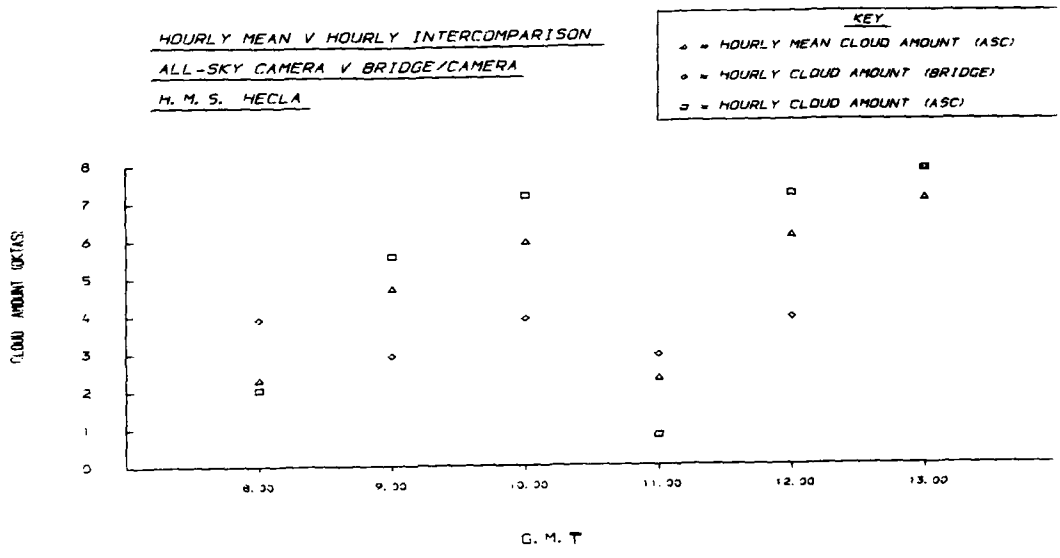

Figure 46 Hourly mean (all-sky camera), hourly sampled (all-sky camera), hourly (bridge) total cloud for August 22nd 1978

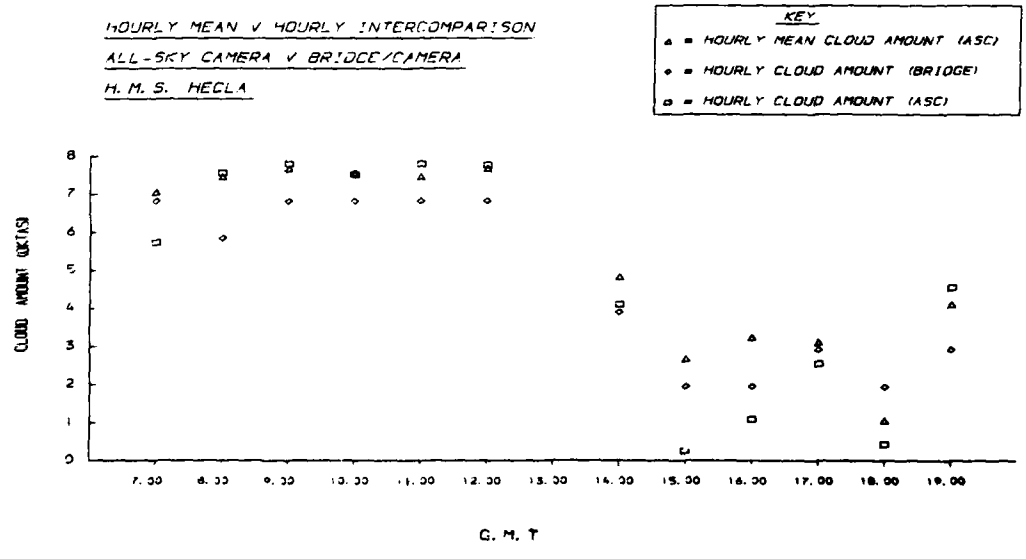

Figure 47 Hourly mean (all-sky camera), hourly sampled (all-sky camera), hourly (bridge) total cloud for August 24th 1978

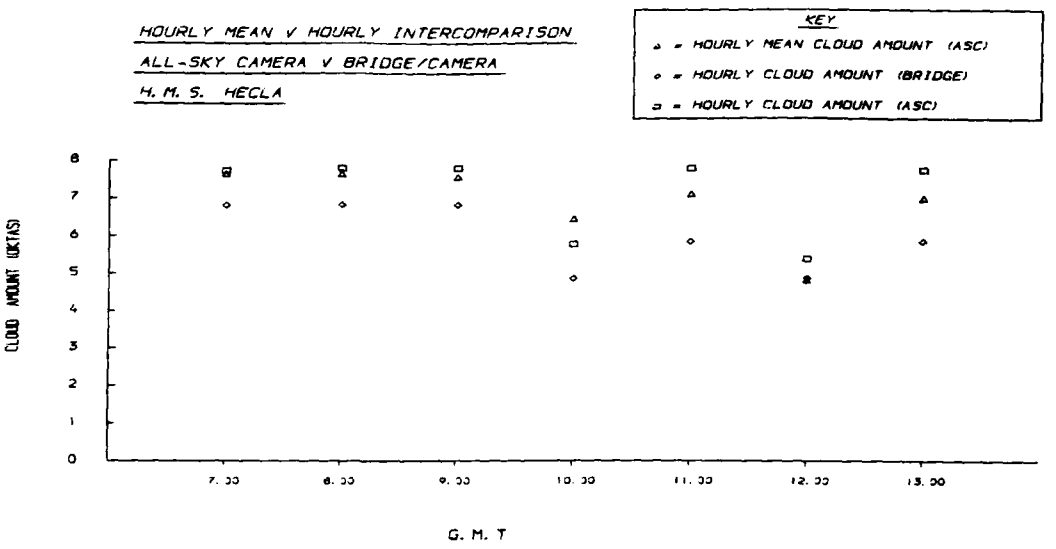

Figure 48 Hourly mean (all-sky camera), hourly sampled (all-sky camera), hourly (bridge) total cloud for September 1st 1978

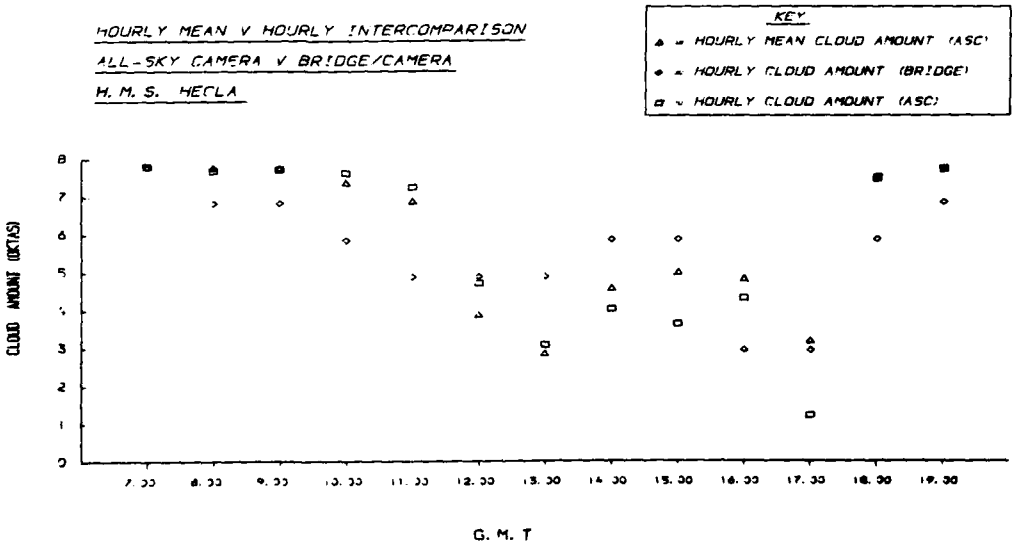

Figure 49 Hourly mean (all-sky camera), hourly sampled (all-sky camera), hourly (bridge) total cloud for September 2nd 1978

3.5 Effects of variability and errors in cloud on the sea surface radiation budget

The corresponding radiation data (short and longwave) will be used to derive estimates of incoming short and longwave radiation using various empirical models that have been developed e.g. Lumb (1964) and Lind and Katsaros (1982). The high temporal resolution of the all-sky camera observations permits estimates to be made every five minutes whereas the actual radiation measurements denote hourly averages. The empirical relations all depend to a certain extent on cloud amount, type and height. Consequently using days of highest temporal variability, hourly means of short and longwave radiation will be estimated in order to observe what effect variable cloudiness has on both quantities. It is also recognised that such calculations are sensitive to errors in the reported cloud amount. Using the results of the previous section, it is hoped to quantify the effect of such errors and to illustrate the advantage of the all-sky camera in making more precise cloud amount estimations.

4. Presentations and Publications

Presentations

The effects of temporal variations of cloud amount and type on estimates of short and longwave radiation at the ocean surface, A.H. Goodman and A. Henderson-Sellers, International Radiation Symposium, Lille, France, 18–24 August 1988 (oral presentation).

Publications

Clouds for climate: recent progress in cloud detection and analysis, A.H. Goodman and A. Henderson-Sellers, *Atmospheric Research*

Global cloud data: problems in synthesis of heterogeneous sources, K. McGuffie, A.H. Goodman and A. Henderson-Sellers, *Proceedings of Twenty-First International Symposium on Remote Sensing of Environment*, 273–288, Ann Arbor, Michigan, October 1977

Regional analysis of 3D Nephanalysis total cloud amounts for July 1983, K. McGuffie, A. Henderson-Sellers and A.H. Goodman, submitted to *International Journal of Remote Sensing*

Climatological contingency probabilities of clouds, A. Goodman, K. McGuffie and A. Henderson-Sellers, submitted to *Journal of Climatology*

The effect of temporal variations of cloud amount and type on estimates of short and long-wave radiation at the ocean surface, A.H. Goodman and A. Henderson-Sellers, *Proceedings of International Radiation Symposium*, Lille, 18–24 August 1988

5. References

Hahn, C.J., Warren, S.G., London, J., Chervin, R. and Jenne, W., 1982, Atlas of simultaneous occurrence of different cloud types over the ocean NCAR TN-201 + STR, NCAR Technical Note, National Center for Atmospheric Research, Boulder, Colorado, 35pp and 68 maps

Hahn, C.J., Warren, S.G., London, J., Chervin, R.M. and Jenne, R.L., 1984, *Atlas of Simultaneous Occurrence of Different Cloud Types Over Land*, NCAR Tech.Note TN-241+STR, 214pp.

Henderson-Sellers, A., McGuffie, K. and Goodman, A.H., 1988, Improved snow and cloud monitoring: new climatological relationships between surface and satellite observations, Final Scientific Report, 1 July 1987 – 30 June 1988, Grant no. AFOSR-87-0195, European Office of Aerospace Research and Development, London

Kasten, F. and Czeplak, G., 1980, Solar and terrestrial radition dependent on the amount and type of cloud, *Solar Energy*, **24**, 177–189

Lind, R.J. and Katsaros, K.B., 1982, A model of longwave irradiance for use with surface observations, *J. Appl. Meteorol.*, **21**, 1015–1023

Lind, R.J., Katsaros, K.B. and Gube, M., 1984, Radiation budget components and their parameterization in JASIN, *Quart. J. Roy. Meteor. Soc.*, **110**, 1061–1071

Lumb, F.E., 1964, The influence of cloud on hourly amounts of total solar radiation at the sea surface, *Quart. J. Roy. Meteor. Soc.*, **90**, 43–56

Pollard, R.T., 1978, The Joint Air–Sea Interaction Experiment — JASIN 1978, *Bull. Amer. Meteor. Soc.*, **59**, 1310–1318

Sèze, G., Drake, F., Desbois, M. and Henderson-Sellers, A., 1986, Total and low cloud amounts over France and Southern Britain in the summer of 1983: comparison of surface-observed and satellite-retrieved values, *Int. J. Remote Sensing*, **7**, 1031–1050

World Meteorological Organisation, 1974, *Manual on Codes*, **Volume 1**, (WMO Publ., No 306), WMO, Geneva